TANGENTIAL FLOW ULTRAFILTRATION AS AN ANTIFOULING STRATEGY FOR WATER QUALITY SENSORS

TANGENTIAL FLOW ULTRAFILTRATION AS AN ANTIFOULING STRATEGY FOR WATER QUALITY SENSORS

By

PANKAJ SAINI

B. Tech. (Mechanical Engineering)

A Thesis

Submitted to the School of Graduate Studies

In Partial Fulfillment of the Requirements

For the Degree

Master of Applied Science

McMaster University

MASTER OF APPLIED SCIENCE (2017) McMaster University

Mechanical Engineering Hamilton, Ontario, Canada

TITLE	TANGENTIAL FLOW ULTRAFILTRATION AS AN ANTIFOULING STRATEGY FOR WATER QUALITY SENSORS
AUTHOR	PANKAJ SAINI
SUPERVISOR	Professor P. R. Selvaganapathy Department of Mechanical Engineering
NUMBER OF PAGES	xviii, 124

Abstract

Water quality monitoring is important for water treatment facilities, food processing industry, aquaculture and in geological surveys. Gathering reliable measurements from sensors can be challenging over extended periods of time in conditions where the biological growth occurs. This is due to biofouling, the growth of biotic matter, on the sensor surface. This deteriorates the quality of measurements from the sensors over time.

Among the several important parameters for water quality monitoring are the pH and the dissolved oxygen (DO) content of the water that plays a major role in its overall quality. The water monitoring sensors are susceptible to biofouling on its surface which affects the performance. In severe biofouling conditions the effect is evident in a matter of days or even hours. Several methods have been used to control biofouling. However, each method has its own disadvantage and there is no universal solution.

In this thesis, membrane technology was implemented to prevent the biofouling on the sensor surface by filtering out the bacteria from the water sample. First, the effects of accelerated biofouling on the microfabricated pH and DO sensors were studied. The sensors were placed in accelerated biofouling conditions for a period of one week and the sensor response was quantified periodically. Both the pH and DO sensor lose their

sensitivity over the duration of the experiment. A decrease of 21% in the sensitivity value is observed for the pH sensor and a decrease of 66% in the sensitivity value is noted for the DO sensor.

Next, the sensors were integrated in a customized flat sheet Tangential Flow Filtration (TFF) device with an ultrafiltration membrane and placed on the permeate side of the filtration device. It was noted that integrating the sensors with the TFF device helps in controlling the deterioration in the sensor performance in accelerated biofouling conditions. The decrease in the sensitivity noted for the pH and DO sensors used with TFF were 5 times lower as compared to when used without the TFF device.

Additionally, spacers of different shapes were tested with humic acid solution as feed to compare the membrane fouling. Using image analysis, it was shown that grooved spacer with staggered herringbone shape is useful in mitigating membrane fouling. The decline in permeate flux over the period of the experiment was 71% with the grooved spacer, while a decrease of 88% was noted with conventional flat channel spacer.

In summary, the device proposed in this thesis was shown to successfully prevent the deterioration of sensitivity of the microfabricated pH & DO water monitoring sensors by preventing the formation of biofilm on the sensor surface and the grooved spacers used in the TFF helped in mitigating membrane fouling. The final chapter concludes with recommendations for further development of the device and suggestions for future work.

The recommendations are directed towards the development of the device for carrying out in-situ measurements, such as, insertion of reference electrode with the sensing electrode in the bottom part of the device and provision of inlet and outlet for buffer solution. Some future studies are also suggested such as investigation of the effect of membrane fouling and the effect of pressurized conditions on the quality parameters of the water samples.

Acknowledgement

It was an excellent opportunity to work with Dr P. Ravi Selvaganapathy and I wish to express my gratitude for his guidance and availability at all times. He provided a flexible working environment and has been incredibly supportive throughout my master's. Besides that, he has been a wonderful teacher. I have learned valuable teachings from him and for that I truly admire him.

My sincere gratitude goes to Dr Jamal Deen and Dr Raja Ghosh for the constant encouragement and for providing access to facilities in Micro & Nano Systems Lab and Bio-Separations Lab, respectively.

I would also like to thank Dr C.Y. Ching for the critical feedback in the group meetings.

I am thankful to Yiheng, Leo and Si Pan for several valuable discussions, ideas and for all the help and support they provided me in the last two years. Special thanks to Rahul Sadavarte for his feedback on this thesis.

I am grateful to all my lab mates in Centre for Advanced Micro-Electro Fluidics for all the help during my stay here. It was an excellent environment to work, and to have fun. I would also like to acknowledge the support from the technicians Mark, John and Michael for assistance with the fabrication of several devices.

Finally, I would like to thank my parents for providing unconditional support always. To them, I shall forever be indebted.

Table of Contents

List of Figures

List of Tables

Chapter 1

Motivation and Organization

1.1 Motivation

Biofouling is one of the main factors that prevents long-term deployment of the water monitoring sensors to obtain reliable data [1]. It is defined as the undesirable accumulation and subsequent growth of micro-organisms, plants or animals on a surface [2] [3]. Biofouling of the water monitoring sensors leads to unreliable measurements of water quality parameters due to the formation of biofilm on the sensor surface [4]. Biofouling can grow at the expense of biodegradable substances present in the medium which causes the formation of biofilm on the sensor surface and leads to inaccurate measurements [5]. It a significant obstacle in long-term use of sensors for accurate data collection [6] [7].

Current antifouling methods for water monitoring sensors, ranging from surface wiping to chemical treatments, are not suitable for the microfabricated sensors as these methods result in damage to the sensor surface and degraded response. The cost-effective microfabricated sensors used for water monitoring sensors require methods that do not cause any mechanical abrasion on the sensing surface. Therefore, a method is required

that prevents the formation of biofilm on the surface of the sensors without degrading the microfabricated sensor's surface which will help in obtaining accurate measurement of the desired water quality parameters over longer periods of time.

1.2 Objective

This research is directed towards developing a system that conforms to the following requirements -

a) It should be environmentally-safe. The system should not leech harmful materials into the environment.
b) Prevents the contact of particulate matter and bacteria onto the sensor surface as this would prevent the formation of the preliminary layer for biofouling
c) Does not change the ionic & chemical composition of the sample, which ensures precise measurements of water quality parameters such as pH and DO (dissolved oxygen). This would prevent inaccurate measurements.
d) It should be economical. It should provide long-term continuous operation with minimal need for replacement, repair as well as maintenance

To meet the above requirements, membrane technology was implemented in this study. A customized tangential flow filtration device with a flat sheet ultrafiltration membrane was integrated with advanced low-cost pH and DO (dissolved oxygen) sensors to prevent the formation of biofilm on the sensor surface. The ultrafiltration membrane

helps in removing the solid matter and microorganisms like bacteria from the water sample and provides permeate as the sample to the sensor without changing the composition of the initial sample. The tangential flow configuration helps in extending the life of the filtration membrane by maintaining filtration of the sample over a longer period as compared to the conventional normal flow filtration configuration.

1.3 Organization

The thesis is organized in the following chapters:

Chapter 2 provides an overall background for the importance of water quality monitoring and the important water quality parameters. The issue of fouling of the water monitoring sensors is introduced. The different stages of the fouling are described. Current strategies that are implemented to control fouling on the sensors are explained in detail with their respective advantages and disadvantages. The chapter ends with a summary.

Chapter 3 presents the device design, the working concept, and the experimental set up. Membrane filtration technology is also introduced. The device, which is a custom Tangential Flow Filtration module with an ultrafiltration membrane, is described in detail with design and its fabrication. List of materials that are used in the study is provided with details. Finally, the experimental setup is described and the procedure for taking the measurements is explained.

Chapter 4 presents the experimental data obtained from the pH and DO sensors integrated in the Tangential Flow Filtration (TFF) device. The experimental results include the data from the sensors kept in different working conditions and are presented as the change in response. The study of fouling on the ultrafiltration membrane in the TFF is also presented. Different channel spacer designs are compared for the extent of fouling with humic acid as the feed solution. Image analysis shows reduced fouling on the membrane with the grooved spacers as compared to the conventional flat channel spacer. Finally, the spacer with staggered-herringbone groove is implemented in the TFF device with accelerated bio-fouling solution and is shown to have enhanced filtrate flux.

Chapter 5 concludes with the contribution of the research study. Future work is suggested in the end.

Chapter 2

Introduction

2.1 Water Quality Monitoring

Water is an essential resource for humans. We need quality water for drinking, agriculture, aquaculture and in industrial settings such as food processing and manufacturing industries. The quality of water is of immense importance for not just human health and but also for the environment sustainability. The quality of surface water governs the aquatic life. Hence, precise and reliable water quality measurement is essential for varied purposes.

The critical parameters for monitoring the water quality include pH, DO (dissolved oxygen), Temperature, Conductivity and Turbidity measurement [8] [9] [10]. Among these parameters, temperature, pH and DO values of the water sample directly affect the rate of microbial growth in the water body [11] [12] [13]. If these parameters are allowed to change in an uncontrolled manner it may have adverse effects [7] [10] [13]. Monitoring of these parameters helps to predict the possibility of contamination and, is a preventive measure to take necessary action promptly.

2.1.1 pH and its importance

pH is the measure of acidic or basic nature of the sample and is one of the most important operational water quality parameters [15]. At a given temperature, the intensity of the acidic or basic property of the water, indicated by the pH, is defined as the negative logarithm of the hydrogen ion activity [16].

$$pH = -\log_{10}[H^+];$$

WHO guidelines advises the pH of drinking water to be maintained between 6.5 to 8.5 [17]. Based on the review from Health Canada, the proposed guidelines gives the acceptable pH range of drinking water between 7 to 10.5 [12].

The pH level of water affects other water characteristics such as temperature, the levels of dissolved organic carbon, the alkalinity, buffering properties of the water; and microbiological characteristics like biofilm [12].

pH can have a major influence on water chemistry, which will also significantly affect the treatment processes, like coagulation and disinfection [18] [19] [20] [21]. It is an important parameter in the formation of disinfection by-products, its effects vary from one by-product to another [17]. Therefore, it is important to monitor and control the pH during drinking water treatment so as to maximize treatment effectiveness and efficiency [22] [23] [24]. Also, it is necessary in the distribution system to control corrosion and reduce leaching from distribution system and the pipeline components [12] [25] [26]. The

control of pH in the distribution system is necessary to minimize corrosion and exposure to metals such as lead [12]. Higher pH (up to 10.5) in the distribution system helps in lowering concentrations of lead and other metals [12].

2.1.2 Dissolved Oxygen content and its importance

Dissolved Oxygen is an important component of surface water for the maintenance of aquatic organisms that use aerobic respiration [27]. Oxygen is moderately soluble in water and the solubility is governed by a set of physical conditions including atmospheric and hydrostatic pressure, salinity, turbulence and temperature [28]. The DO (dissolved oxygen) content in water is largely controlled by the balance between input of oxygen and consumptive metabolism. Oxygen enters the water from the atmosphere through diffusion. It is also produced by aquatic plants and algae as a by-product of photosynthesis [29]. Dissolved oxygen is mainly consumed in the respiration of aquatic organisms, respiration of aerobic bacteria and microbes with decomposition of organic matter like algae, leaves and fish, and in chemical reactions such as the reduction of nitrate (NO_3) to ammonia (NH_4) in the water bodies [29].

It is important to monitor the DO levels in wastewater management as it helps in aerobic processes involved in the treatment [27]. The concentration of dissolved oxygen in fresh water varies and depends on the atmospheric pressure, temperature as well as

salinity [30]. The oxygen saturation values in fresh water varies between 7ppm and 14ppm under normal conditions [30].

Traditional water quality monitoring involves collecting the samples from the source and transporting the samples for laboratory based tests for various water quality parameters. There are several drawbacks of this method such as deterioration of samples over time, limited time monitoring and limited samples. On the other hand, the continuous water quality monitoring has the benefit of having the sensing technologies in the water source itself. These methods are briefly described in Figure 1. With advances in electronics and power management systems, now biofouling is the main factor that limits the time for which a water quality instrument can be deployed in field for continuous monitoring.

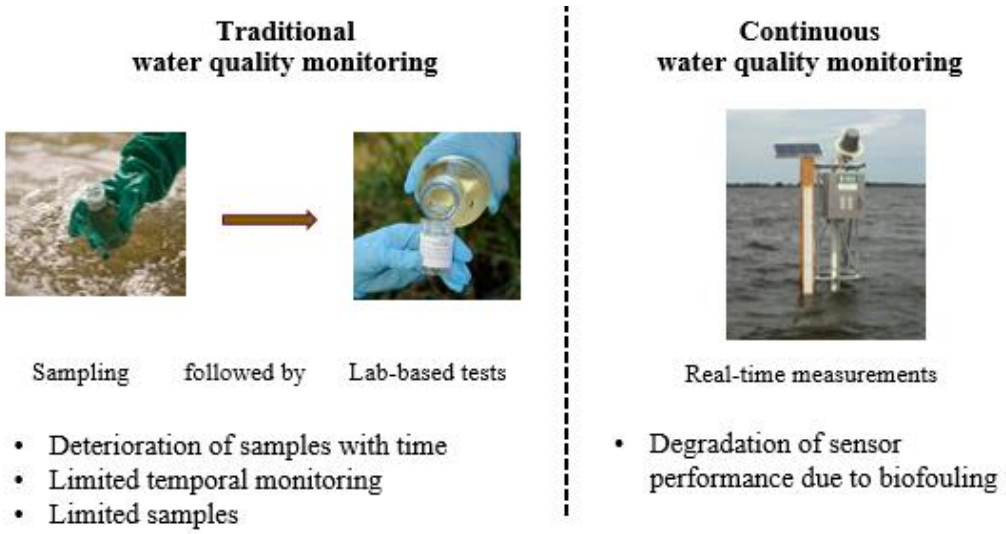

Figure 1 Traditional and continuous water quality monitoring [31] [32] [33]

2.2 Biofouling

Fouling is the deposition of unwanted material on a surface which is detriment to its function [34]. The fouling is classified based on the fouling material. The deposition of living organisms is known as biofouling and the deposition of non-living substances can be inorganic (mineral deposits, corrosion, crystallization, etc.) or organic (natural organic matter) fouling [34].

Biofouling is defined as the undesirable accumulation and growth of living organisms on a surface [2] [35]. It is one of the major engineering challenges that affects a variety of industries [13] [35] [36]. As opposed to inorganic fouling which is due to deposition from corrosion, crystallization and suspended particles, biofouling is due to the growth of living organisms on a surface which aided by the consumption of the biodegradable nutrients available in water [35] [37] [38]. The type and degree of fouling largely depends on the local environment, and the microbial presence. These parameters vary significantly between medical, marine, industrial and water monitoring applications [6] [35] [39]. The definition of biofouling includes both microbial fouling (due to micro-organisms) and macrofouling (due to macroscopic organisms) [5]. Generally, medical and water monitoring applications involve the microbial fouling and the marine and industrial settings are prone to macrofouling and inorganic fouling in addition to microbial fouling [23] [35] [40] [41]. It is important to prevent the formation of biofilm

on the sensor surface not only to get accurate and reliable measurement but also to increase the lifetime of the sensor [42] [43] [44][45].

Continuous water monitoring over a long time to get reliable data is challenging. This is because the water monitoring sensors are susceptible to fouling in the form of biofilm i.e. the unwanted growth of microorganisms on the surface or due to deposition of biological matter [2] [8]. The biofouling of the sensor surface causes degradation in the sensor performance over time and decreases the lifespan of the sensors [4] [46]. Moreover, surface water represents sources of multiple types including rivers, lakes, etc. and each water body has a different composition and different levels of pollution. This can make accurate water monitoring further difficult due to large spatial variation in its properties, especially if the water body has significant variation in the amount of nutrients and biodegradable matter [47]. The presence of biodegradable matter and nutrients in the water promotes the growth of microorganisms on a solid surface immersed in the water and accelerates biofouling. Water monitoring sensors used in conditions that promote biofouling are more prone to degradation in performance.

For water monitoring purposes, biofouling in the form of microbial fouling is one of the major obstacle in the long term use of the sensors [6]. The formation of biofilms reduces performance of sensors by insulating the surface of the electrode by multiple ways, including, inhibition of mass transfer [6]. As opposed to abiotic type of fouling that

includes scaling and particle fouling, biofouling is a special case because the foulant i.e. the microorganisms, grow at the expense of nutrients or the biodegradable substances from the water, converting them into metabolic products and biomass [5]. Hence, the foulant micro-organisms can multiply and grow in number. In the process of growth they produce extracellular polymeric substances (EPS), which keeps them together and holds them to the surface and also add to the fouling [5].

It is necessary to control fouling on the sensor surface because the fouling can create an artificial environment around the sensing surface and the measured values would not be true representative of the sample [2]. Also, the biofouling makes the water monitoring sensors susceptible to frequent replacement in order to obtain reliable data for longer periods of time.

2.3 Stages of biofouling

Biofouling on a surface immersed in water and the subsequent growth of the biofilm on the surface is a complex phenomenon and much remains yet to be understood [48].

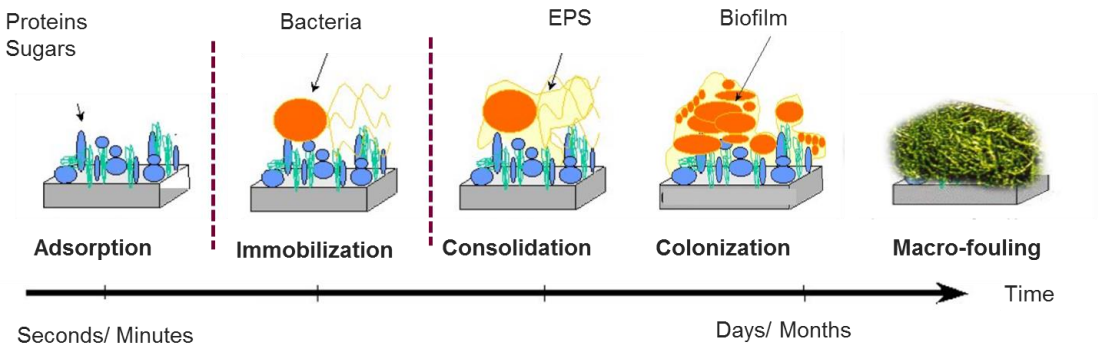

Figure 2 Stages of biofouling 1) Adsorption 2) Immobilization 3) Consolidation 4) Colonization 5) Macro-fouling [48]

However, five main stages of biofouling are identified. Figure 2 shows the different stages of biofouling [48]. It starts when a solid surface being immersed in a media that contains nutrients in the form of proteins, polysaccharides, etc. In a matter of few minutes/hours of immersion of the solid surface in the water it is covered with a layer of organic molecules like sugars and proteins [2]. This is shown in Figure 1(1) and is the adsorption stage. The layer is known as the primary film and unavoidable in most circumstances [48].

The next stage, i.e., immobilization is the transport of microbial cells to the surface, and bacterial immobilization on the surface. At this stage, the adhesion of the bacteria and other microbes forms a very thin layer on the surface. This is shown in Figure 1(2).

The third stage, i.e., consolidation can be seen in Figure 1(3). At this stage the bacterial attachment to the substrate is built up through extra-cellular polymer (EPS) production, forming a microbial film on the surface. Bacteria in the biofilms are meshed within a gel matrix made of EPS [5].

The fourth stage, i.e., colonization is as shown in Figure 1(4). This stage corresponds to the development of a more complex community with the presence of multicellular species [8], [48]. In this stage the microbes adhere to each other leading to thickening of the biofilm.

The last stage, i.e., macro-fouling as depicted in Figure 1(5), is the attachment of macro organisms such as macro algae, mussels, and other such forms of macro organisms. Macro fouling is commonly associated with marine environment, where significant aquatic growth can occur on the surface of underwater structures [35].

2.4 Current antifouling strategies

This sections enlists the current methods used to control the fouling of the water monitoring sensors. There are currently several methods to control fouling in water monitoring sensors. However, each method has some drawback and there is no universal solution. The anti-fouling strategies are described as following.

2.4.1 Mechanical methods

Mechanical antifouling methods include the approaches that implement physical cleaning of the sensor surface by mechanical means. It is either done with the help of water jets or with the use of wipers or scrapers, which is implemented in some of the commercial water monitoring sensors [2] [8] [49] [50]. It can be good for cleaning sensor platforms; however, the major drawback of this method is that the mechanical forces can damage or destroy the sensory elements of the sensors which are exposed to the sample.

Other mechanical methods include the use of piezoelectric material integrated with the housing of the sensor. When and electric potential is applied to the housing, it vibrates upon excitation which helps in removing fouling material from the surface of the sensor [51]. However, high power consumption makes it unsuitable for remote battery-powered systems [8] [51].

Coating the sensor surface with a piezoelectric material was also studied as an anti-biofouling measure [52]. Again, the drawback of this method is high power requirement which makes it unsuitable for use in remote battery-powered sensors. Also, it has been noted that the sensitivity of the sensor decreases due to the coating.

Some commercial sensors uses mechanical means to expose the sensor only for limited duration [53]. This is done with the help of an apparatus in which a sensor is

placed in a protective housing which is above the water level. The housing can be lowered at required time intervals [54].

2.4.2 Biocide generation system

Antifouling paints based on compounds such as tributyltin (TBT) were used extensively used for preventing biofouling in the last few decades. These are made by the reaction of tri-organotin derivatives of acrylic or methacrylic acid and co-polymerizable monomer in the presence of a free radical initiator [2]. Carboxylate bond between the organotin and the polymer backbone can be easily hydrolyzed water, which eliminates any fouling organisms that adhere to its surface [2]. However, tributyl-tin compounds are shown to have hazardous effects on the environment due to which the use of TBTs have been banned from use in antifouling paints since 2003 [55] [56] [57].

Copper, which also has biocide properties is currently used for protecting sensors against biofouling [2] [8]. The Cu^{2+} ions interferes with enzymes on cell membranes, thereby preventing the cell division and hence prevents biofouling [58]. The drawback to this method is that copper is not completely efficient as a biocide on its own. This is because some of the microorganisms, such as some common algae are tolerant to copper [59]. For this reason, it is used with biocides like zinc pyrithione, diuron, etc. but there is little data available on effects of these chemicals on the marine environment [2].

2.4.3 Chlorination

One of the other common techniques used as antifouling for sensors is chlorination [8]. Chlorine is used as a disinfectant. When added to water chlorine produces hypochlorous acid and hypochlorite ion which can kill pathogens such as bacteria and viruses by attacking the lipids in the cell walls and destroying the structures inside the cell. Chlorine helps in preventing the growth of biofouling on the surface as it kills the micro-organisms and hinders their growth [36]. The drawback of chlorination is that the by-products of chlorine in water are carcinogenic compounds like trihalomethanes [60] [61].

2.4.4 Irradiation

The use of ultraviolet light for irradiation has also been used for preventing biofouling on surfaces such as sensors, membranes, valves etc. as well as for disinfection of wastewater [2] [62] [63]. The advantage of UV irradiation is that it helps in preventing the release of toxic products in the environment of the sensor.

Laser irradiation has also been studied for preventing biofouling [64] [65]. Low power pulsed laser was irradiated on the biofouling organisms like marine diatom species like Skeletonema costatum and Chaetoceros gracilis. It was observed that there was increase in mortality of these biofouling organisms, up to 97.7+/-3.1% in the case of

Skeletonema costatum and up to 98.9+/-0.6% in the case of Chaetoceros gracilis, respectively with increasing laser energy density and duration of irradiation [64] [65].

Ultrasonic irradiation has also been widely used for controlling biofilm formation [66] [67] [68] [69]. It has been shown to enhance the efficiency of biocides in removing the bacteria on the surfaces. In one study, 20 kHz ultrasound applied for one minute for a total of three times after an equal interval of 24 hours, was beneficial in reducing the thickness of biofilm from 24μm to 16μm [67]. Ultrasonic waves used in combination with enzymes was useful removal in the amount of biofilm by 61-96% [70].

Low frequency mechanical vibration was also studied as an antifouling measure. It is noted that in combination with vibration it helps in preventing the macro organisms settling on the exposed surface [2].

However, the irradiation methods are not practical solutions for incorporation in remote sensors because of energy requirements [2].

2.4.5 Electrochemical methods

Electrochemical methods are another alternative as antifouling measures. One of the methods used is the electrolysis of seawater, i.e., electro chlorination which helps in generation of hypochlorite. This has been widely studied as a method for prevention of fouling of marine sensors [2] [71]. This is done with the use of an electrode placed close

to the sensor or by conductive coating on the sensor surface. The major drawback of this method is that the coating can degrade over time by the application of potential [71].

Another approach that uses electrochemistry is the direct use of electrons to destroy the microorganisms instead of generating a biocidal substance. TiN electrode has been used to prevent fouling using this method [2] [72]. Materials like graphite-silicone have also been used for fabricating such electrodes [47].

Boron-doped diamond (BDD) is another such material which is resistant to biofouling to some extent and is inert at high potential [4] [6] [73]. It is a versatile electrochemical material. These properties of BDD have been utilized to develop a free chlorine sensor that enables electrochemical cleaning of the sensor surface in situ using high potentials [6].

Electrically conductive polymer-nanocomposite nanofiltration membranes have been shown exhibit antifouling properties when tested in highly bacterially contaminated LB media [74]. Alternating electrical current was applied to the membrane which efficiently prevented biofouling [74].

The use of copper screening as an electrolytic grid is another method for the prevention of fouling [75]. Although it is beneficial in controlling macrofouling, it is very expensive to initially install.

2.4.6 Summary

In this chapter, the basis for the thesis is introduced. The importance of biofouling prevention for water monitoring sensors is explained. The current antifouling methods in use are described in detail. The current methods either use harsh treatments not suitable to microfabricated sensors or require chemical coatings which are not environment friendly. Hence, a cleaner and easy-to-operate technology is required to prevent the formation of biofilm on the sensor surface and its subsequent deterioration in performance due to the biofilm. An ideal method for preventing biofouling should have following characteristics-

1) It should be environmentally-safe.
2) It should prevent the contact of particulate matter as well as biofouling microbes onto the sensor surface
3) It should not inherently affect the water quality parameters to be measured
4) It should be a cost-effective method and should provide long-term operation with minimal need for replacement, repair, and maintenance

Chapter 3

Device Design and Experimental Setup

The previous chapter explained the need for anti-biofouling measures for water monitoring sensors and the current antifouling methods in use. This chapter will focus on the design of the device used in this study to prevent biofouling on microfabricated pH and DO (dissolved oxygen) sensors and the experimental set up used. First, a brief background is given about membrane technology, which was implemented in this study. This is followed by the design and fabrication of the filtration device and the experimental setup. The device presented in this thesis a Tangential flow filtration (TFF) module used with an ultrafiltration membrane. It is integrated with advanced, microfabricated pH and DO (dissolved oxygen) sensors, with the sensors placed on the permeate side of the filter. The complete system comprises of the TFF device and a peristaltic pump on a common platform. It is shown to successfully prevent the deterioration of the sensor performance over time due to fouling on the sensor surface in accelerated biofouling conditions.

3.1 Membrane Technology

Membrane processes involve the use of semipermeable membrane of definite physical and chemical properties to separate particles or molecules primarily on the basis of size, shape, and chemical composition [76]. It is an emerging technology that has gained a lot of popularity because of its diverse and increasing applications in various large-scale industries covering water purification, milk purification, food processing, desalination, energy storage (in fuel cells), wastewater treatment, microorganisms separation and so on [77]. This has been possible due to the advancement in the performance of the membranes, accelerated by the developments of novel membrane materials with better chemical, thermal and mechanical properties as well as a wide range of selectivity [77] [78] [79]. Stimulated by these developments there has been a significant decrease in the operational costs of membrane processes which has made membrane technology one of the most promising technologies for this century [9] [77].

This section provides a brief overview of the Membrane Technology, its advantages, and applications. It is followed by the design of the device used in this study, which implements the use of membrane technology.

3.1.1 Membrane & Membrane Operations

A membrane, when associated with separation or purification processes, is essentially defined as a barrier to separate two phases and be able to restrict the transport of various components in a selective manner [77].

The membranes can be classified on multiple criteria such as the membrane material, the membrane morphology, geometry, and applications. Figure 3 shows the general classification of the synthetic membranes [80].

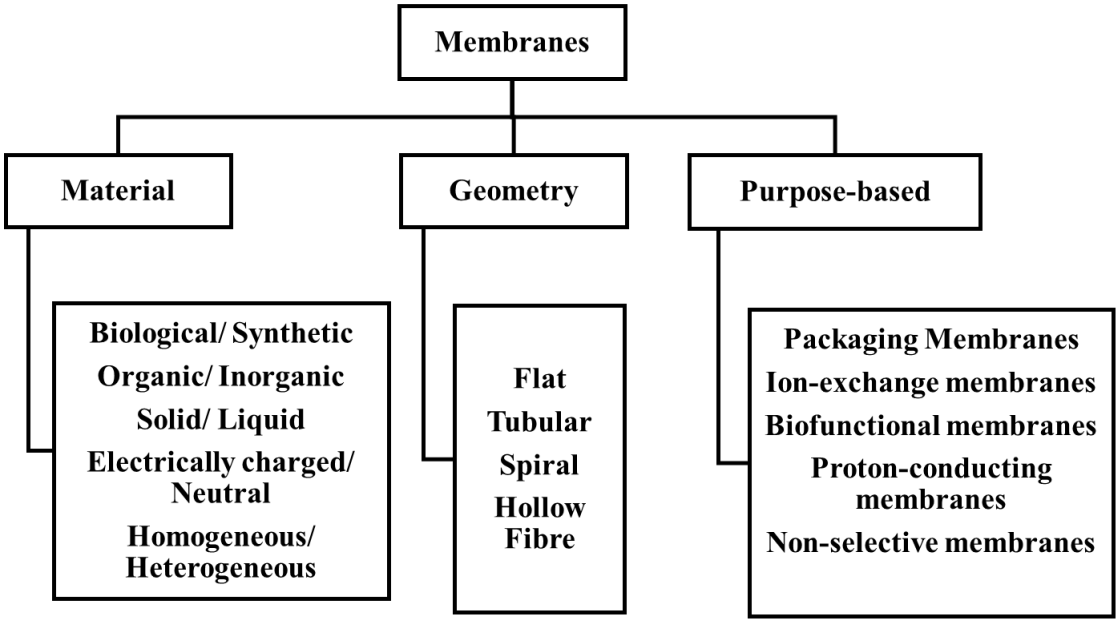

Figure 3 Classification of membranes based on membrane material, geometry of the filtration channel and purpose of use [81]

Membranes can be classified on the type of materials. These materials can be either biological or synthetic. Biological membranes are found in nature. These membranes form cells and enables separation between inside and outside of organisms [82] [83]. Biological membranes are composed of lipids, proteins and sugars [83]. Synthetic membrane, also known as artificial membranes, are used in laboratories and industries for separation purposes [81]. These membranes are made from materials such polymers and inorganic materials such as metals and ceramic [79]. Synthetic membranes are widely used in industries for microfiltration, ultrafiltration and reverse osmosis [84]. Liquid membranes are the synthetic membrane that are made from non-rigid material like emulsion liquid membranes, molten salts, etc. and are used in wastewater treatment for removal of organic compounds [85].

The membrane comes in different geometry and can be classified as flat, tubular, spiral, and hollow fiber membrane. Flat sheet membranes are made with a membrane cast on the surface of a flat support material. Flat sheet membranes can be used either as a single sheet or in multiple stacks and easy to install and maintain. Tubular membranes are suitable for handle viscous liquids with high levels of suspended solid and are generally used in modules of stainless steel or plastic. Spiral membranes consist of tightly packed filter material that is placed between mesh spacers and wrapped in a tube. Spiral membranes provide more surface area in than tubular membranes. Hollow fiber

membranes consist of extruded fibers with a small hollow portion. Filtration in hollow fiber membranes can be either from inside the fiber to the outside or in the reverse direction. These membranes have low cost per unit area but are easily fouled [86]. These are generally employed in industrial water, wastewater, and food/juice processing applications suited to the high production demands [77].

Membrane can also be classified based on the specific purpose they are used for such as proton exchange membranes for fuel cells, ion exchange membranes for physically or chemically modifying the permeating components, bio-functional membranes for bio-separations, packaging membranes to prevent permeation, etc. [81].

Membrane separation processes differ based on separation mechanisms and size of the separated particles. Figure 4 gives an overview of the fundamentals of the membrane processes.

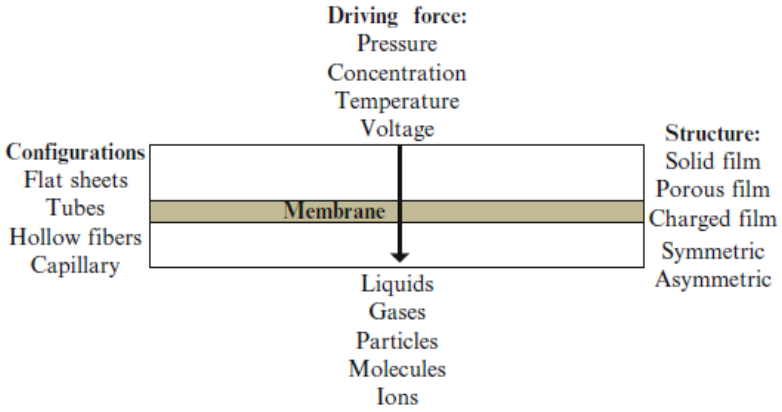

Figure 4 Fundamentals of membrane and membrane processes [77]

Based on the driving force of the operation, the membrane operations are classified in the following four categories-

a) Pressure driven operations, such as Microfiltration, Ultrafiltration, Nano filtration, Reverse Osmosis
b) Concentration driven operations, such as dialysis
c) Operations in an electric potential gradient, such as electro dialysis
d) Operations in a temperature gradient, such as membrane distillation

This study targets to prevent the contact of solid particulate matter and micro-organism like bacteria with the surface of water monitoring sensors by the physical removal of the solid particulate and biological matter from the feed water sample. Pressure is used as the driving force in membrane separation when the process is based on particle size and does not involve a gradient of concentration, potential or temperature to drive the separation. Pressure-driven processes, such as ultrafiltration and microfiltration are extensively used in biopharmaceutical and water treatment industries to remove bacteria and organic matter [87] [88]. These processes are classified based on the pore size of the membrane and are shown in Figure 5.

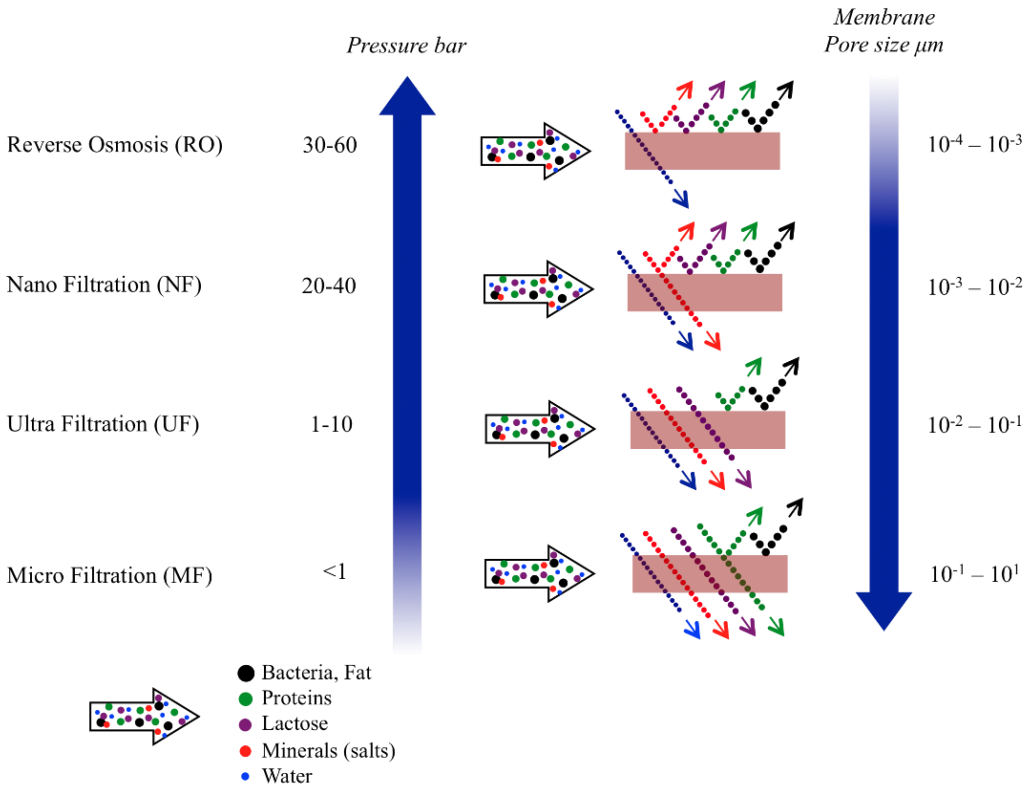

Figure 5 Pressure driven membrane processes- Microfiltration, Ultrafiltration, Nano Filtration and Reverse Osmosis, with their respective pore-size and working pressure ranges [89]

Figure 5 shows the different pressure driven membrane processes categorized based on the pore size of the membrane. The figure shows the pressure ranges at which these processes are carried out.

3.1.2 Applications of Membrane Technology

Membrane technology has wide range of applications in a variety of fields and their numbers are expected to continually increase [80] [81] [84]. The uses include but not limited to water treatment, dairy purification, desalination, waste- water reclamation, food processing, gas and vapor separation, air pollution control, industrial waste treatment, hemodialysis, proteins, and microorganism separation, etc. [1]. The applications of membrane technology are briefly categorized in following main applications-

a) Water Treatment

Membrane separation is one of the advanced wastewater treatment technologies and has been playing an important role in lower pollutant levels in purifying and/or concentrating a wide variety of fluids from water and wastewater to pharmaceutical and chemical products [9]. Low pressure-driven membrane processes are becoming increasingly attractive as an alternative to conventional water and wastewater treatment [90]. This is because, the low-pressure membranes can possibly shorten and streamline the entire treatment process chain by eliminating coagulation, flocculation and sedimentation processes, and have been considered as an alternative for conventional drinking water treatment [91]. It is one of the advanced wastewater treatment technologies and has been playing an important role in lower pollutant levels in purifying

and/or concentrating a wide variety of fluids from water and wastewater to pharmaceutical and chemical products [34].

Increase in water quality regulations and decrease in availability of fresh water supplies has made membrane processes a widely favorable and an increasingly important process in drinking water treatment [92].

b) Food Processing

Besides water treatment, pressure driven membrane processes are used widely in food processing [93]. In food industries membrane separation, microfiltration and ultrafiltration utilizes microfiltration and ultrafiltration for purification of fruit juices [94]. It is applied to whey processing in the production of proteins for commercial use and thus transforms a waste by- product into a valuable product using this process [95]. It is also used in the production of the fermented food products where membranes filtration has established itself for the clarification of wine, beer and vinegar and based on its now proven reliability in other production steps [94].

c) Pharmaceutical Industry

In the pharmaceutical and biotechnology industries, membrane technology is used for ultrapure water for a range of application such as preparation of tissue culture, buffer solutions, analytical solvents, drug and intravenous solutions [77]. Efficient membrane

separation processes are also to obtain high-grade products in pharmaceutical industries to remove or recover toxic or valuable components from industrial effluents [96].

3.1.3 Flow geometries in Membrane Filtration

The membrane filtration is mainly carried out in two configurations- dead-end filtration (also known as normal flow filtration) and tangential flow filtration (also known as crossflow filtration) [77] [97]. Figure 4 shows the schematic of the two types of configurations.

As seen in the Figure 6, in the dead-end filtration the flow is normal to the membrane surface whereas in the tangential flow filtration the flow of the feed is tangential to the membrane surface.

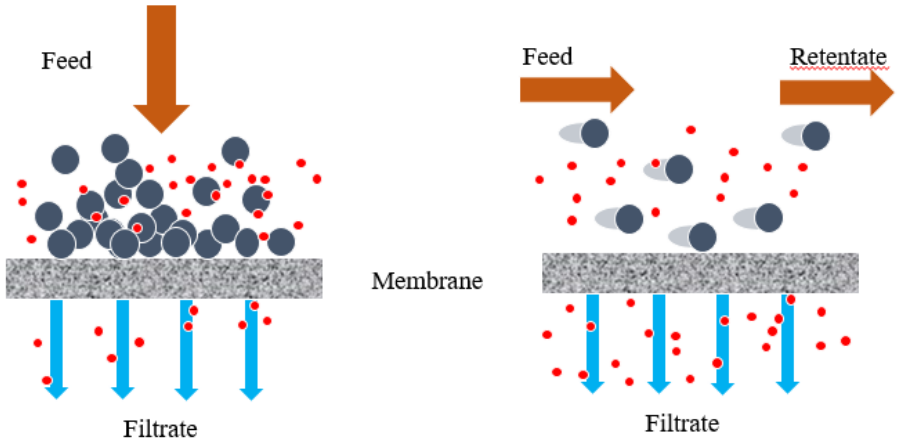

Figure 6 Schematics of dead end filtration and tangential flow filtration [77]

In dead-end filtration, the entire feed flow moves towards the membrane perpendicularly such that the retained particles and other components get accumulated [77]. This lead to clogging of the membrane pores and the deposition of the particles on the membrane surface [77]. In the tangential flow filtration, the feed stream flows in a parallel direction to the membrane surface [77]. Only a portion of the feed stream passes through the membranes under the driving pressure [77].

The main limitation of pressure-driven membrane processes is the reduction of the flux with time to a value far below the theoretical capacity [34] [98]. Typical variation of the permeate flux with time is an initial rapid decrease which is then followed by a long and gradual decline over time [34]. Membrane fouling is one of the main phenomena responsible for the permeate flux decline [34][99]. Out of the two modes of filtration- dead end filtration and the tangential flow filtration, the latter has a significant benefit for long term operation [84]. Moving the feed flow tangentially to the membrane surface helps in getting higher permeate flux as the feed stream continuously removes the material from the membrane surface. Membrane fouling is always lower as the flow in the tangential direction itself provides cleaning action due to the shear forces acting on the membrane surface [77]

3.2 Device Design

The water quality sensors are susceptible to biofouling which causes the deterioration of their performance over time. The biofouling is caused due to the growth of microorganism on the sensor surface. It is desired to control the biofouling on the sensor surface to increase the life time of the water monitoring sensors and obtain reliable data for longer periods of time. The target of this study is to prevent the fouling on the sensor surface. For this, it is desired to remove solid and biological matter from the water samples and to provide the treated sample to the water monitoring sensors. At the same time, the ionic composition should not change so that water quality parameters could be measured precisely.

As mentioned in the objective of this study following criteria were considered for the design of the device-

1) Prevents the contact of particulate matter as well as microbes onto the sensor surface
2) Does not change the ionic & chemical composition of the sample, which ensures precise measurements of water quality parameters like pH and DO (dissolved oxygen) values
3) Provides long term continuous operation with minimal need for replacement, repair as well as maintenance

To satisfy the above criteria, membrane technology was utilized to prevent the deposition of particulate matter and microorganism which subsequently leads to biofouling. As explained in the previous section, membrane technology can be helpful in physical removal of solid and biological matter from the water sample. The following sections explains the device design in detail.

3.2.1 Membrane Selection

Fouling is the deposition of unwanted material on a surface which detriments it's function [34]. The fouling is classified based on the fouling material. The deposition of living organisms is known as biofouling and the deposition of non-living substances can be inorganic (mineral deposits, corrosion, crystallization, etc.) or organic (natural organic matter) fouling [34].

Biofouling is the unwanted accumulation and growth of living organism on the surface [2] [35]. The biofouling on the surface of the sensors is caused by the biological matter present in the water including microorganisms which grow on the surface of the sensors. Thus, it is necessary to filter out these biological matters from the sample that goes to the sensors.

The smaller the pore size of the membrane, the higher is the quality of the permeate and lesser probability of the microorganisms passing the membrane. However, with the decrease in the pore size of the membrane the Trans Membrane Pressure (TMP)

required to maintain the same level of permeate increases significantly [81]. Keeping these restrictions in consideration, PES (polyethersulphone) ultrafiltration membrane (Product code: OT300SHEET, Pall Corporation, USA) with a higher pore size, 300kDa was chosen for the filtration device. PES membranes are recommended for filtering bacteria, cell media, etc. as it has very low protein binding and gives faster flow rates than cellulosic or nylon membranes.

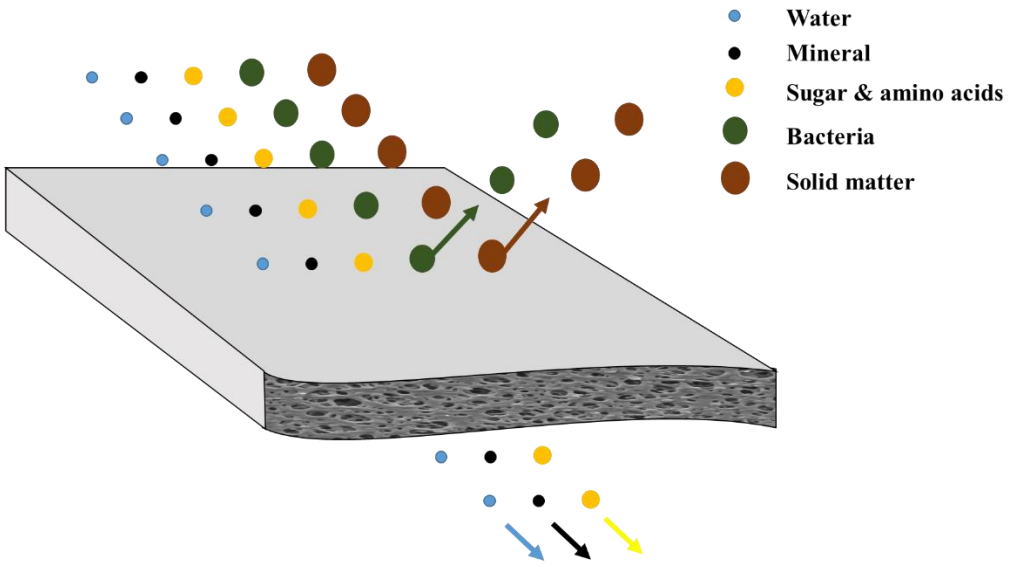

Figure 7 Representation of ultrafiltration membrane showing the effective removal of different particle sizes from feed stream

Figure 7 shows an illustration of the effective removal of different particle sizes using an ultrafiltration membrane. The pore size of 300kDa corresponds to ~35nm on a linear dimension scale [100]. It is small enough to prevent the bacteria from passing

through the membrane as they fall in the size range of 500nm to 10µm. The smaller pore size is chosen as it helps to prevent not only bacteria but also larger biomolecules from passing through the membrane. The initial stage of biofouling is the adsorption i.e. when nutrients in the form or polysaccharides and sugars get adsorbed on the surface. This contributes in the formation of biofilm as this stage is followed by the transport, immobilization, and colonization of bacteria on the surface.

3.2.2 Flow configuration

The two modes of membrane filtration are explained in section 3.1.3. Dead-end (normal) filtration clogs over a period of time and the trans membrane pressure required to maintain the permeate flux is significantly higher as compared to tangential mode of operation. On the other hand, Tangential flow filtration (TFF) is a filtration technique in which the feed passes tangentially along the surface of the membrane.

For the flow configuration, tangential mode was selected as the tangential flow of the feed helps in removing the particles that adhere on to the membrane surface during the separation process. Tangential mode helps in cleaning the membrane due to shear forces induced by the flow along the membrane surface and maintains a higher permeate flux for longer period of time as compared to the dead-end filtration. TFF is typically used in separation of cells (cell harvesting), separation of target molecules, separation of components based on the molecular size and for concentration of the product solution by

the removal of solvent and small molecules. Unlike normal filtration which involves the feed passing only once through the membrane, TFF can be used for the recirculation of the retentate. In this study, TFF mode is implemented to the prevent the solid particulate matter and bacteria from passing through the membrane.

3.2.3 Device design

The objective of the device design was to have a portable system which can be easily deployed in the field to prevent biofouling on the water monitoring sensor. In this study, the pH and DO sensor are integrated in the TFF device and placed on the permeate side of the membrane to prevent the degradation of the sensors performance in accelerated biofouling solution. Additionally, a spacer with staggered herringbone shaped grooves was used to study its effect on membrane fouling with the help of image analysis. The two main components required such a portable system are the pumping mechanism and the tangential flow filtration device. These are described as below-

1) Pumping mechanism-

A peristaltic pump was used as the pumping element in this device. These are positive displacement pumps and are widely used in laboratory set ups as the pressure source for a variety of fluids. These pumps do not cause any contamination, as the fluid is never exposed directly to any part of the pump. However, commercial peristaltic pumps are very expensive and bulky, which makes them unsuitable for use in a portable system.

A compact, lightweight and a cost-effective OEM peristaltic pump was obtained (Product number 200-330-012-050, Williamson Manufacturing Company, West Sussex, UK) and was used to pump the feed to the TFF device. This compact peristaltic pump can provide a flow rates up to 400ml/min.

2) TFF device-

This is the main part of the system that comprises of the membrane and the sensors (integrated on the permeate side of the membrane). It provides feed filtered through the membrane to the water monitoring sensors. A polyethersuphone (PES) ultrafiltration membrane of 300kDa was selected in this study. The selection of the membrane is covered in section 3.2.1. The TFF process is controlled by an interplay of several operating parameters according to the specific process requirements and the two most important factors are the feed flow rate and the trans membrane pressure. The membrane surface area determines how much feed can be handled in a process run. For ultrafiltration, the typical values of feed 100-200L of feed per m^2 of membrane surface area and higher values are considered for cost-effective processes [81][101]. Accordingly, the membrane area selected for this study was $20cm^2$.

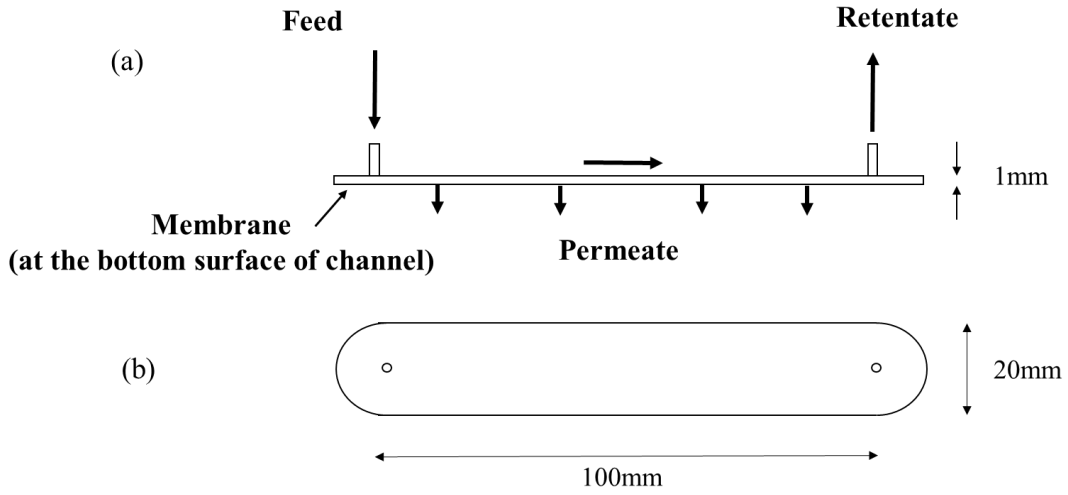

Figure 8 (a) Front and (b) top view of the channel inside the TFF. Dimensions are shown in mm and the directions of the feed, retentate and permeate are indicated

Figure 8 shows the front and the top view of the channel in the TFF device. The sensors used in this study are Pd/PdO based pH sensor and hemin based DO sensors. The sensing area of the sensors used is 5mm x 10mm. The channel width is kept as 20mm to accommodate sufficient number of sensors across the channel. The height of the channel was kept as 1mm A feed flow rate of 150mL/min was selected for the experiments. This corresponds to a velocity of 12.5cm/s in the channel, with Reynold number (R_e)~250. It was desired to have a low flow rate to study the effect of the grooved channel spacer on the membrane fouling as compared to conventional flat channel, at low R_e number flow.

For finding the optimum trans membrane pressure (TMP), a test was carried out DI water and 1% yeast extract as the feed for the TFF device with varying TMP values.

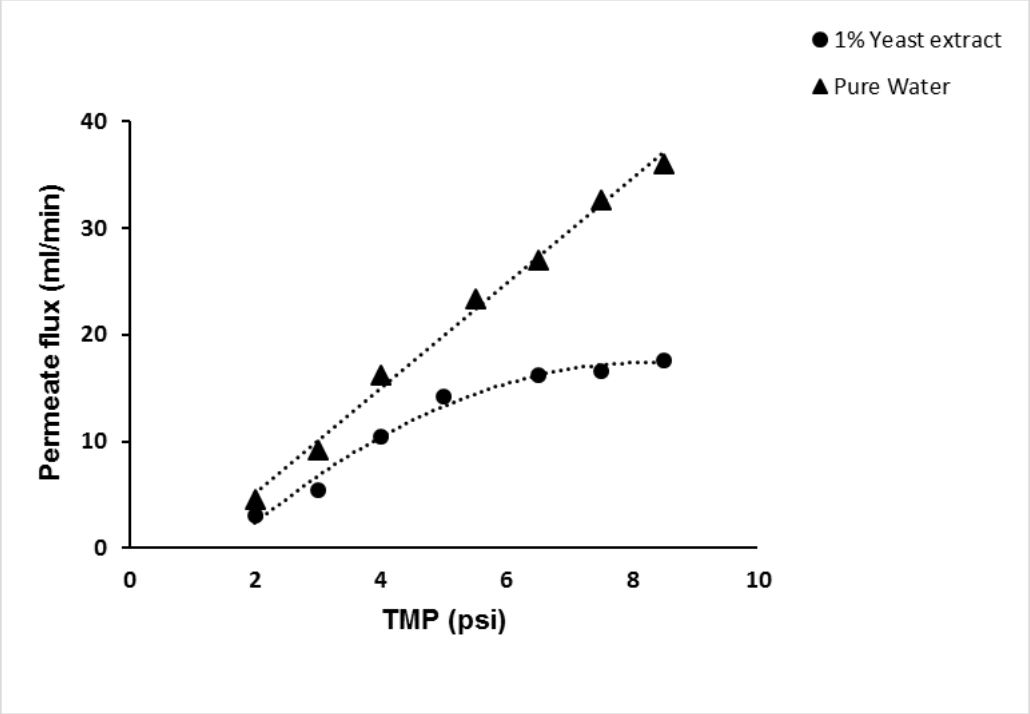

Figure 9 Permeate flux (mL/min) vs TMP (psi) with DI water and 1% Yeast extract as feed to find the optimum range of TMP

Figure 9 shows the permeate flux variation with DI water and 1% yeast extract at different TMP. The optimum TMP value range is when any increase in trans membrane pressure causes a large variation as compared to the permeate flux value obtained with DI water. From this test, a TMP value of 5psi was selected. The size and the length of the tubings were determined experimentally to achieve the desired trans membrane pressure range and are listed with details with the experimental set up in section 3.4.1.

3.3 Device Fabrication

Based on the design criteria and analysis above the device was fabricated. This section covers the material used, the fabrication process and the assembly of the device.

3.3.1 Materials Used

The material used in the fabrication of the device are listed below.

a) Acrylic

Poly (methyl methacrylate) also known acrylic was used to make the top and bottom part of the tangential flow filtration device used in this study. The acrylic sheets of 12 mm thickness were used.

b) Connectors

Connectors were purchased from Qosina (Ronkonkoma, NY). These were used to attach the tygon tubings to the device, the pressure gauges, and the peristaltic pump.

3.3.2 Fabrication

The device was fabricated with the help of laser cutting and machining. Figure 10a, b &c shows the spacer, the bottom part, and the top part of the device respectively. The dimensions of are mentioned accordingly. The spacer was made from 1mm thick Teflon sheet and was cut with the help of laser cutting.

The acrylic was first cut into rectangular pieces with the help of laser cutting using Speedy 300, Trotec laser machines (Mississauga, Canada). Machining was then carried out to make the inlet and the outlet on the top part. Slots were made on the bottom part of the device to place the pH and the DO sensors. An outlet for the permeate was made on the bottom part as well.

(a)

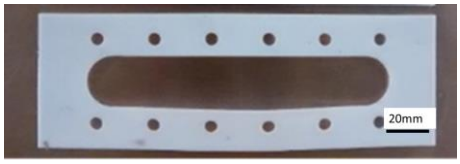

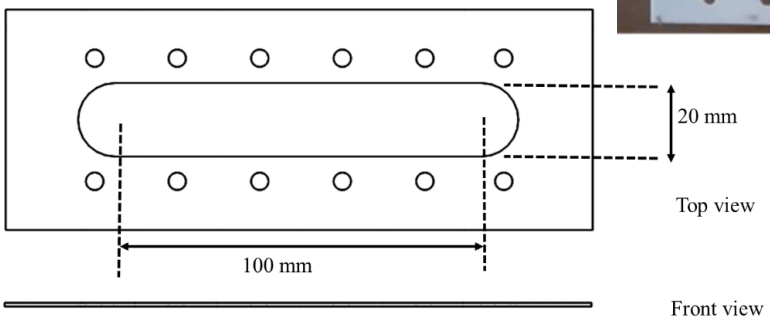

(b)

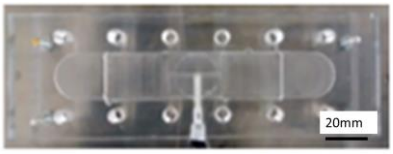

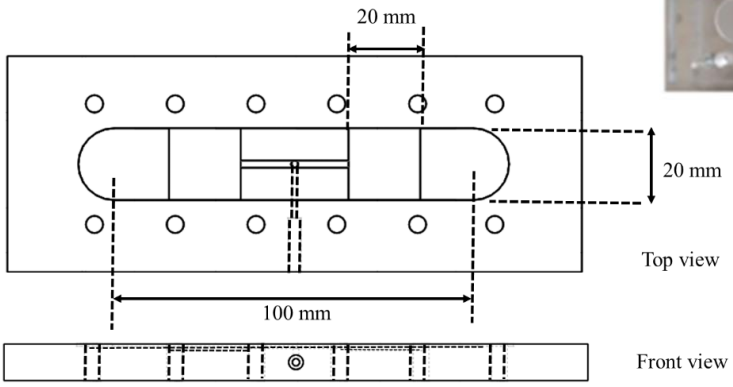

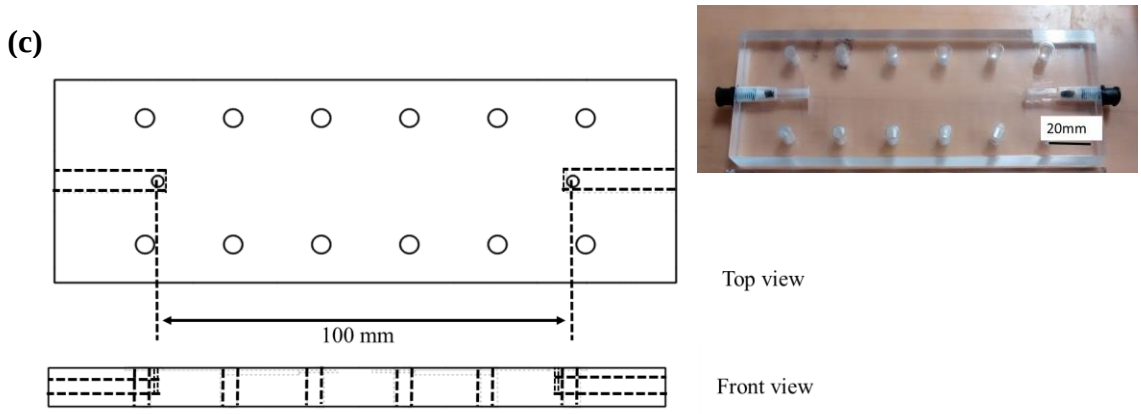

Figure 10 a) Schematic and image of the spacer b) Schematic and image of the bottom part showing the 20mm x 20mm slot for the pH and the DO sensors c) Schematic and image of the top part. All the Schematics include 2 views- top & front view for each part. Dimensions are represented in mm.

3.3.3 Device assembly

Figure 11 shows the schematic of different parts of the TFF device.

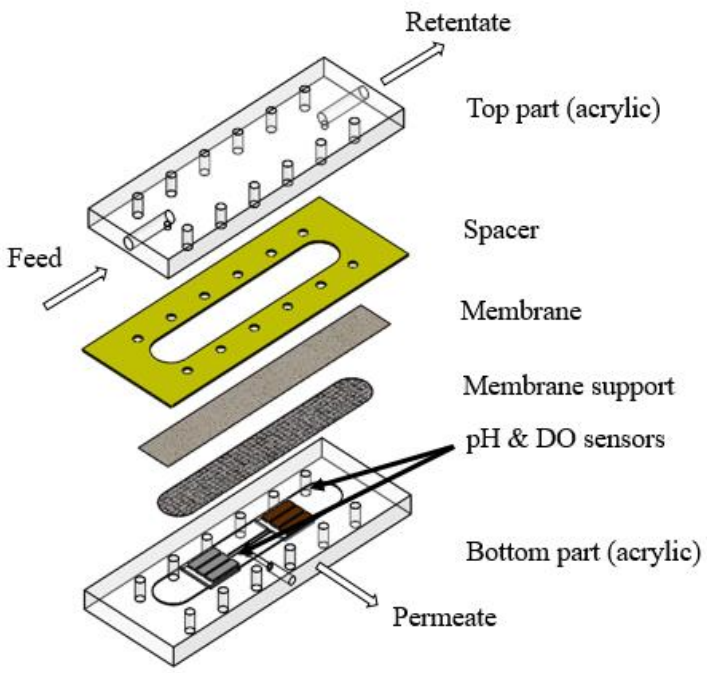

Figure 11 Schematic of the TFF assembly showing different parts of the filtration device and the pH and DO sensors integrated in the bottom part of the device

All the parts were assembled with the help of bolts as shown in the same arrangement as in the schematic after placing the pH and DO sensors in the slots made in the bottom part of the device. This is shown in step-wise manner in Figure 12.

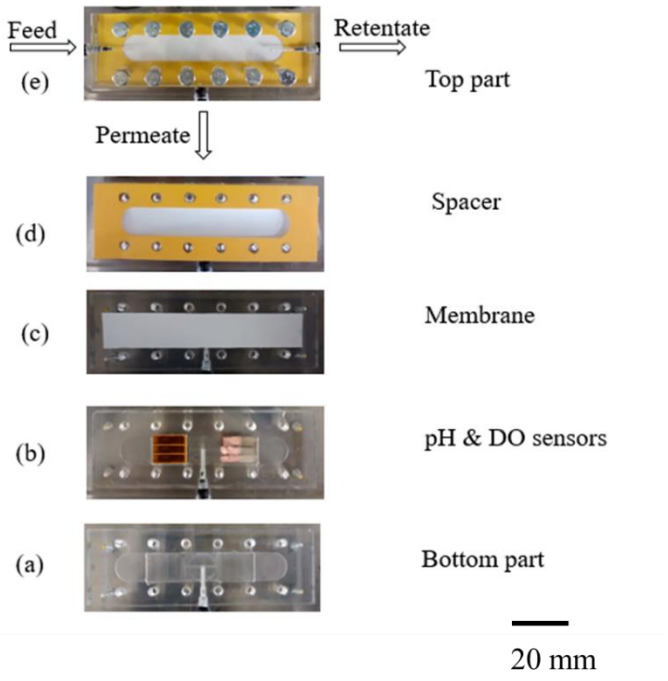

Figure 12 Assembly of TFF (a) Bottom part (b) Placement of pH and DO sensor in the slots on the bottom part (c) Placement of UF membrane (d) Placement of spacer (e) Placement of the top part and assembling using bolts

3.4 Experimental set up

This section explains the experimental set up used in this study. The description of the experimental set up is followed by the description of the materials and equipment used in the experiment.

3.4.1 Experimental setup

The experiment was set up as shown in Figure 13.

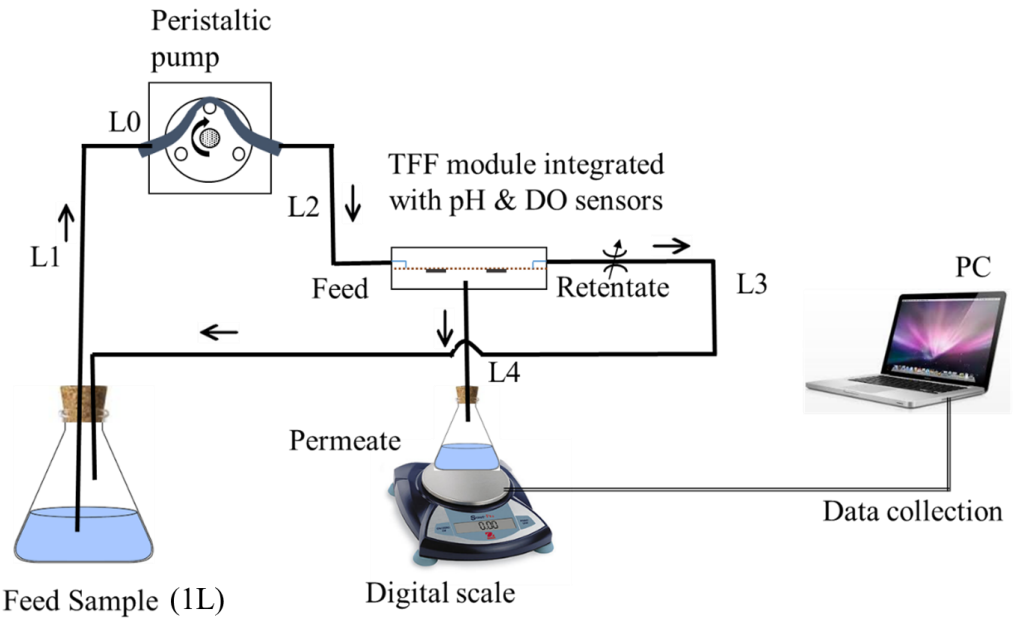

Figure 13 Schematic of the experimental set up showing the TFF device, the peristaltic pump, the feed sample and permeate sample

The Figure 13 shows the schematic of the experimental set up including the TFF device integrated with the pH and DO sensors in it, the feed and the permeate sample containers. The peristaltic pump is used to pass the feed sample over the membrane in the TFF device. Permeate is collected in another beaker and is weighed with the help of a digital scale. The data from the scale is collected on a computer to observe the change of mass with respect to time and to calculate the permeate flux. The tubings used in the experimental set up are listed in Table 1. The size and the length of the tubings were determined experimentally to achieve the desired trans membrane pressure range.

Table 1 List of the tubings used in the experimental set up with their part numbers listed

Tubing	Internal Diameter (mm)	Length (mm)	Type	Part no.
L0	4.8	25	Masterflex platinum-cured silicone tubing	SN-96410-25
L1	2.4	75	Tygon Lab Tubing	RK-06407-73
L2	2.4	25	Tygon Lab Tubing	RK-06407-73
L3	2.4	75	Tygon Lab Tubing	RK-06407-73
L4	2.4	30	Tygon Lab Tubing	RK-06407-73

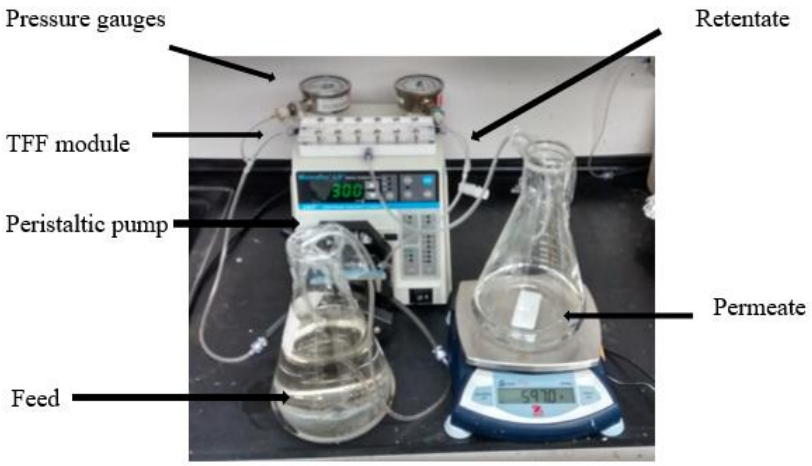

Figure 14 Image of the experimental set up for membrane fouling study using different spacer designs

Figure 14 shows the image for the experimental set up for the experiments carried out to show the integration of the pH and DO sensors with the TFF device when

subjected to accelerated biofouling conditions and for the study of the effect of spacer design on the membrane fouling.

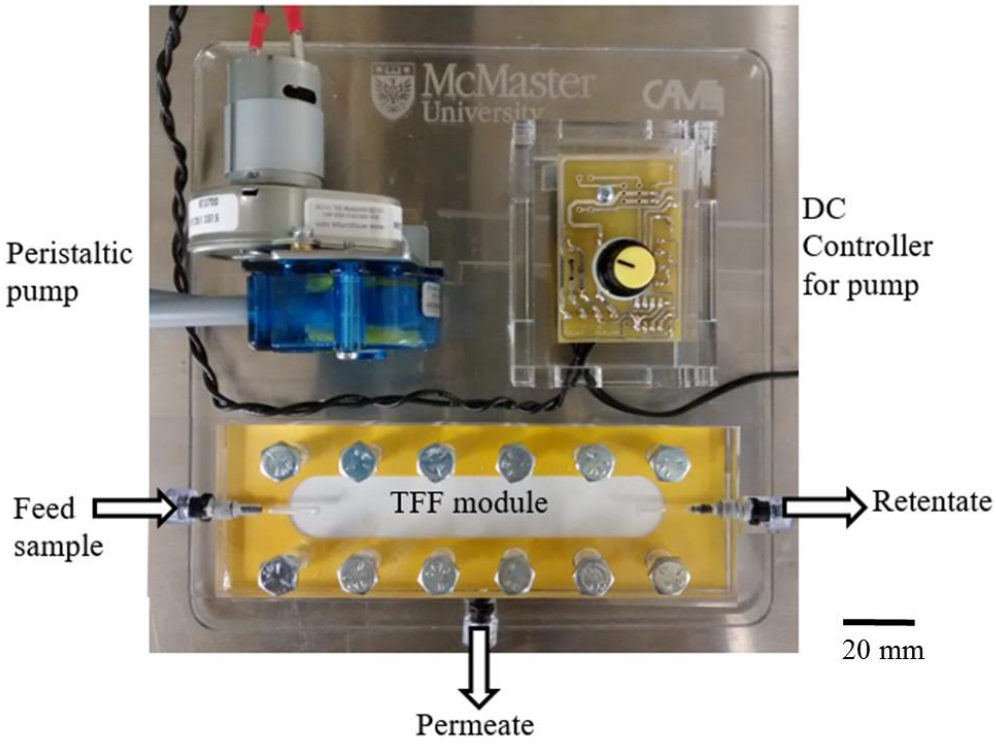

Figure 15 Image of the complete system including the TFF device with the sensors integrated in it and the peristaltic pump with the DC speed controller. The pH and the DO sensors were placed below the membrane (white part seen in TFF device) on the permeate side

Figure 15 shows a portable system that is created on a common acrylic platform of 200mm x 200mm size. It includes the TFF device with the sensors placed on the permeate side of the membrane, the peristaltic pump, and the DC speed controller to control the flow rate of the feed sample. The peristaltic pump was run keeping the feed flow rate as 150mL/min at a trans membrane pressure of 5psi. The pressure gauges (Ashcroft, 30 psi) were used to measure the trans membrane pressure. The system was made to operate for a period of seven days for the experiment and the sensors were taken out of the TFF device prior to taking measurements from them.

3.4.2 Materials

The material used for the experiments in this study are listed as following with a brief description for each.

a) Yeast extract

Yeast extract was purchased from Sigma Aldrich (Product Number: Y1625). It is used for use in microbial growth medium [102]. It is often used in culture media and is the water-soluble portion of autolyzed yeast [102]. It contains amino acids, peptides, water soluble vitamins and carbohydrates as its components [102]. These components act as a source of nutrients for the bacteria to feed on. When added to tap water samples, the bacteria consume these nutrients and grow in number with time.

b) Humic acid

Humic acid was purchased from Sigma Aldrich (CAS Number: 1415-93-6). Humic acid is a product formed of lignin, carbohydrate and protein due to degradation of biological matter [103]. Humic acid is a complex mixture of weak aliphatic organic acids and aromatic organic acids [104]. The molecular size of humic acids (HAs) range from approximately 10,000 to 100,000 Da [104]. It is present in soils and it is often present in surface waters in varying amounts [103]. Its amount varies with the seasons in the water bodies [103]. It is a major constituent of organic matter present in surface waters like ponds, rivers, lakes and ocean [104].

c) Tygon® tubing

Tygon® lab tubings (Product code: RK-06407-73) are flexible polymer tubing which are widely used in chemical processing, laboratory, medical and pharmaceutical industry. It is made of PVC (poly vinyl chloride) based material. Tygon lab tubings were purchased from Cole-Parmer® and used as the inlets and outlets in the experimental set up.

3.4.3 Equipment

The following equipment were used for the experiments in this study.

a) Peristaltic pump

A peristaltic pump was purchased from Williamson Manufacturing Company (West Sussex, United Kingdom), Product number 200-330-012-050. It was used to pump the

feed continuously to the TFF device for filtration. Figure 16a shows the peristaltic pump used in this study. A DC speed controller (6-15V) was fabricated to control the flow rate of this peristaltic pump by varying the motor speed.

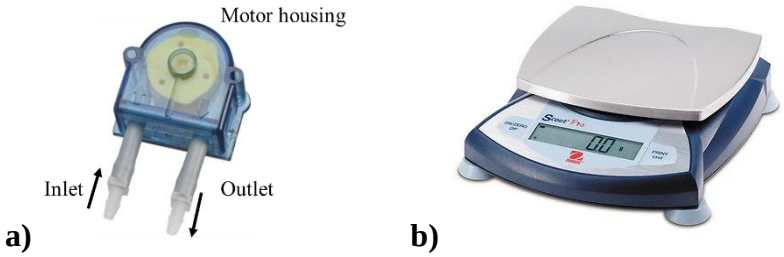

Figure 16 a) Peristaltic pump [105] **b) Weighing scale** [106]

b) Weighing scale

A digital weighing scale Ohaus Scout Pro Portable Electronic Balance (Ohaus), Part no. SP6000 was used to measure the permeate mass flow rate. Figure 16b shows the weighing scale used in this study.

3.4.4 Feed Sample Preparation

The sample used for accelerated biofouling was 1% yeast extract solution. It was prepared by adding 10gm of yeast extract to 1L of tap water in a conical flask.

The humic acid sample was prepared by adding 10mg Humic acid to 1000mL DI water and using an ultrasonic bath for 30 minutes to dissolve the humic acid in the water.

3.5 pH sensor measurements

The pH sensor used in this study was low cost, Palladium/Palladium oxide (Pd/PdO) film based sensor developed by Qin et al [20].

The sensors were fabricated by spin coating Pd precursor solution onto glass substrates and then followed by annealing in ambient air at 200 °C for 48 hours [20]. The glass substrate was then cut into pieces measuring 5mm by 15mm with sensing area of 50mm^2. The size was convenient for the ease of measurement and adequate for insertion in the TFF module. Studies on this sensor have reported that the signal for this sensor is independent of the sensing area when the sensing area is more than 10mm^2 [19]. Hence, the signal obtained from the pH sensors in this study is independent of the sensing area since it was kept as 50 mm^2. A piece of copper sheet was then glued to one end of the sensor with the help of silver based ink to improve contact between the electrode and the connector for taking measurements. This helps to take the measurements conveniently and avoids spikes in the signal due to disconnection when the sensor was moved and placed in different buffer solutions for measurement.

Figure 17 shows the schematic and image of the sensors showing the sensing area and the copper sheet for connection.

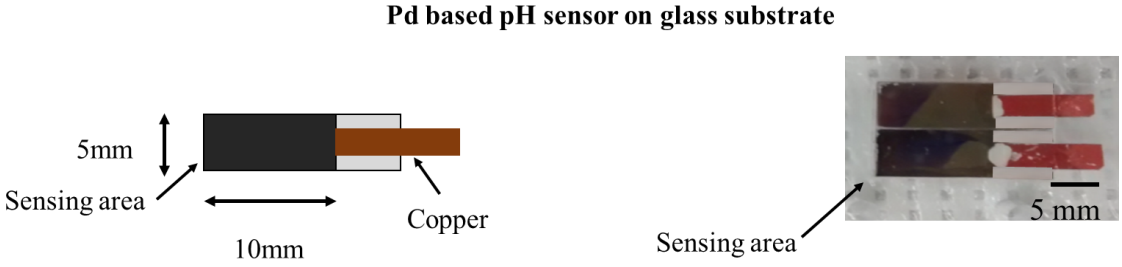

Figure 17 (a) Schematic of pH sensor showing sensing area; (b) Image of pH sensors

3.5.1 Open circuit potential measurement

The open circuit potential measurements were taken for the pH sensor using the set up as shown in Figure 18.

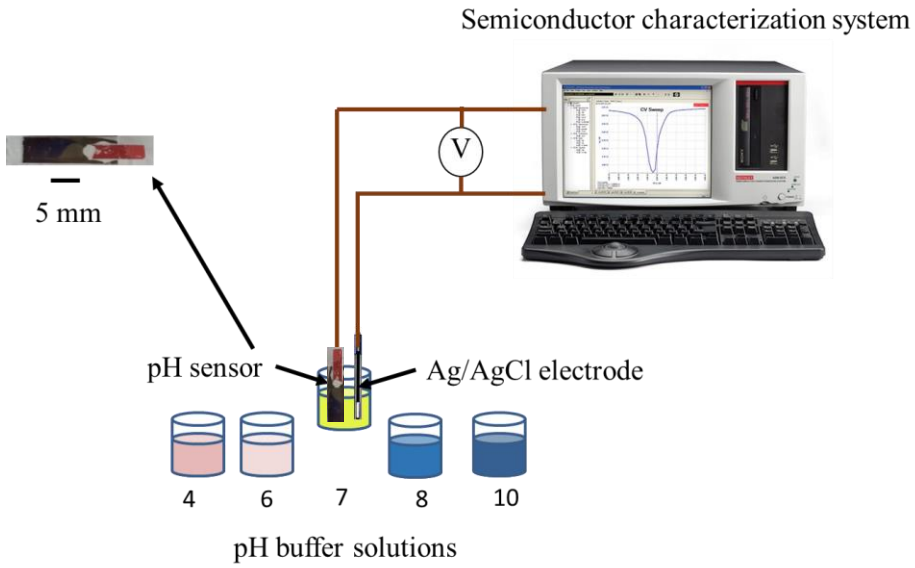

Figure 18 Open circuit potential measurement for pH sensor with buffer solutions of pH=4,6,7,8 & 10 using a semiconductor characterization system. Ag/AgCl was used as the reference electrode.

pH buffers with value of pH= 4,6,7,8 & 10 were prepared by titrating solutions of 0.04M Phosphoric, 0.04M Acetic, and 0.04M Boric Acid, with 0.2N Sodium Hydroxide as described by Briton et al. [107]. These buffer solutions were used to calibrate the sensor. The pH sensor was connected to CPU 1 port system and Ag/AgCl reference electrode was connected to ground electrode port of the semiconductor characterization.

With this procedure, the values of stable voltage were noted for the buffer solution with pH=10, 8,7,6,5 and 4. This cycle was then repeated by taking measurement for the buffer solution with pH value increasing from 4 to pH value of 10. Four such cycles of measurement were performed and were plotted against time as shown in Figure 19. From this process, we get the respective mean values of voltages for the corresponding pH buffer solutions by the given pH sensor.

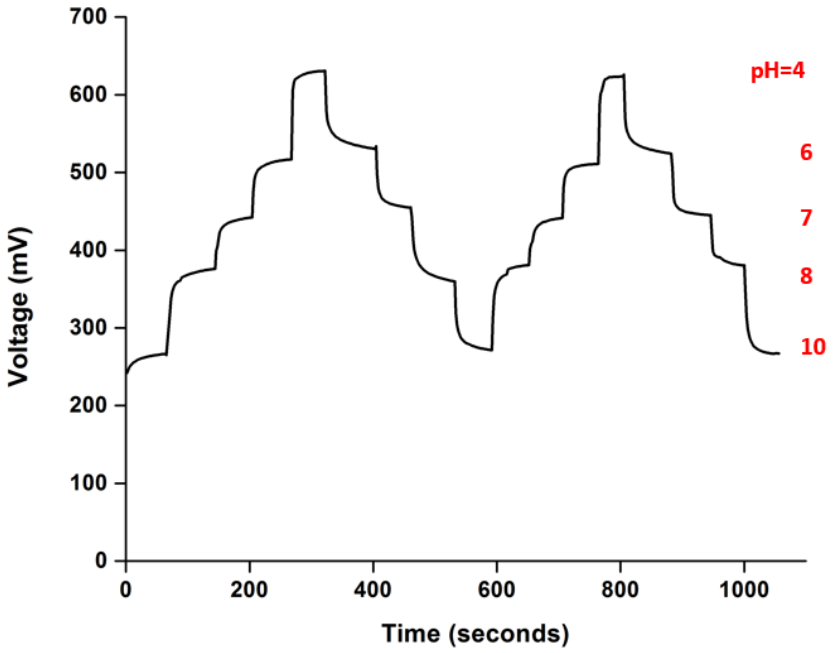

Figure 19 Voltage vs time for pH sensor from open circuit potential measurement. Every step in the voltage curve indicates placing the sensors in different buffer solution for calibration. The buffer solution used have pH values of 4,6,7,8 & 10

3.5.2 Sensitivity calculation

The average values of the voltage were plotted against the corresponding pH value of the buffer solution. The slope of the line in the Voltage vs pH graph gives the value of the sensitivity of the given pH sensor in mV/pH. Figure 20 shows the voltage vs pH plot used to calculate the sensitivity.

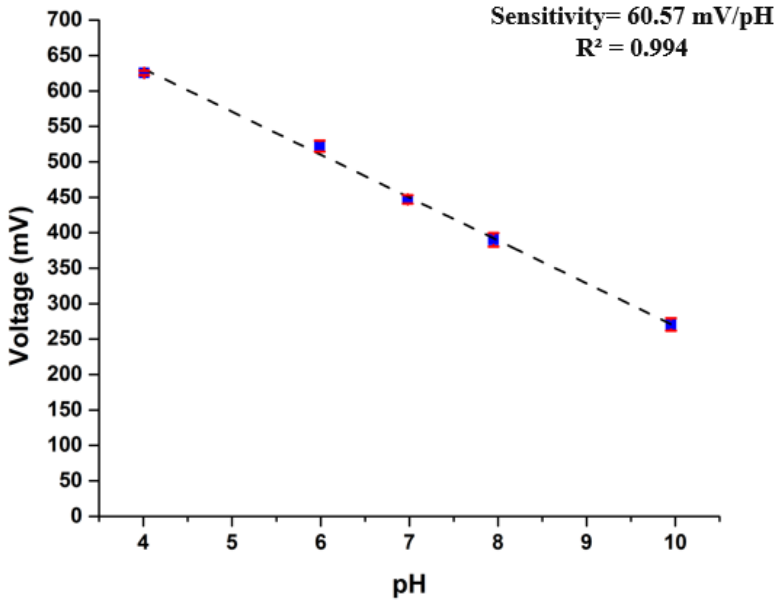

Figure 20 Voltage vs pH graph for Pd/PdO based pH sensors. The slope of the graphs gives the value of sensitivity of the sensor in mV/pH. Error bars are considerably smaller and represent standard deviation (SD)

3.6 DO sensor measurements

The DO (dissolved oxygen) sensor used in this study was an advanced, low cost Hemin based sensor developed by Hsu et al. [108].

The DO sensor was fabricated in multiple steps. First, a 200nm thick layer of electrode, ITO (Indium Tin Oxide) was sputtered on a clean glass substrate. This was followed by annealing the glass substrate at 400 °C for 4 minutes [108]. The glass

substrate was cut into pieces measuring 5mm by 15mm. Electrochemical deposition of hemin was done on the glass substrates using the setup up similar to the figure as shown in Fig with the solution prepared using Chloro [3,7,12,17-tetramethyl-8, 13-divinylporphyrin-2, 18-dipropanoato (2−)] iron(III) (hemin) 98%, pyrrole (98%), silver nitrate (AgNO3, 99%) and Acetonitrile anhydrous, (99.8%) as described in Hsu et al. [108]. This was followed by the deposition of 20µm thick layer of Polydimethylsiloxane (PDMS) by spin coating at 4000rpm for 60 seconds [108].

It was observed that the PDMS starts peeling off from the edges within minutes of operation inside the filtration device due to the shear forces because of the fluid flow. To overcome this, the sensor was covered with Kapton® tape, (DuPont™, Torrance, CA), a polyimide film with silicone adhesive, on the sides to cover the edges and make the sensor more robust while leaving open a sensing area of 50mm^2 on the surface. The sealing on the edges prevents peeling of the PDMS and the electrodeposited hemin layer.

Figure 21 shows the schematic and image of the DO sensors showing the sensing area and the Kapton® tape covering the edges.

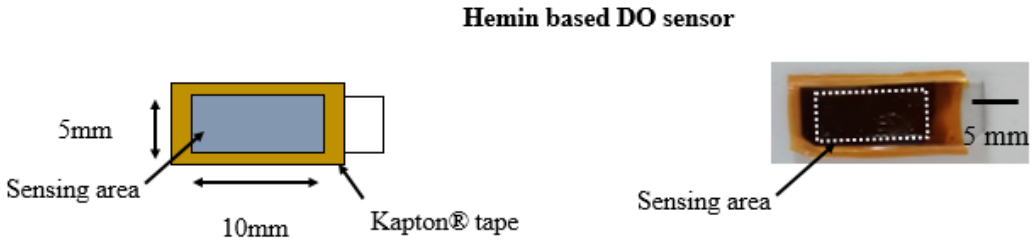

Figure 21 (a) Schematic of DO sensor showing the sensing area (b) Image of DO sensor used

3.6.1 Chronoamperometric measurement

The chronoamperometric measurements for the DO sensor were taken using the set up as shown in Figure 22. The set up consists of Ag/AgCl reference electrode, a platinum wire counter electrode, and the DO sensor as the working electrode. The electrochemical workstation used was EMstat2. Tap water samples with different values of dissolved oxygen content were used for calibration. These samples were prepared by purging nitrogen gas to the sample to lower the DO content and by purging oxygen gas to increase the DO content of the sample used for calibration of the sensor.

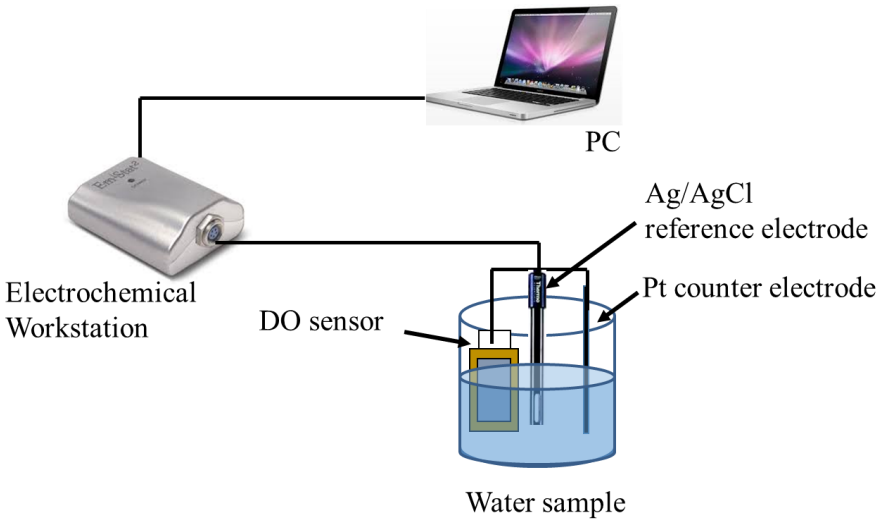

Figure 22 Schematic of experimental set up for chronoamperometric measurement of hemin based DO sensors using water samples with different DO values

The sensor, the counter electrode (Pt wire) and the reference electrode (Ag/AgCl) were immersed in the water sample as shown in Figure 22. Chronoamperometric measurements were performed for the DO sensor for with voltage value of -0.9V time=300seconds [108]. After this time a stable value of current was obtained and was noted against the DO value of the water sample measured using commercial DO sensor. This process was repeated with water samples of different dissolved oxygen content values for calibration. Figure 23 shows the response obtained from the sensors from the chronoamperometric measurements.

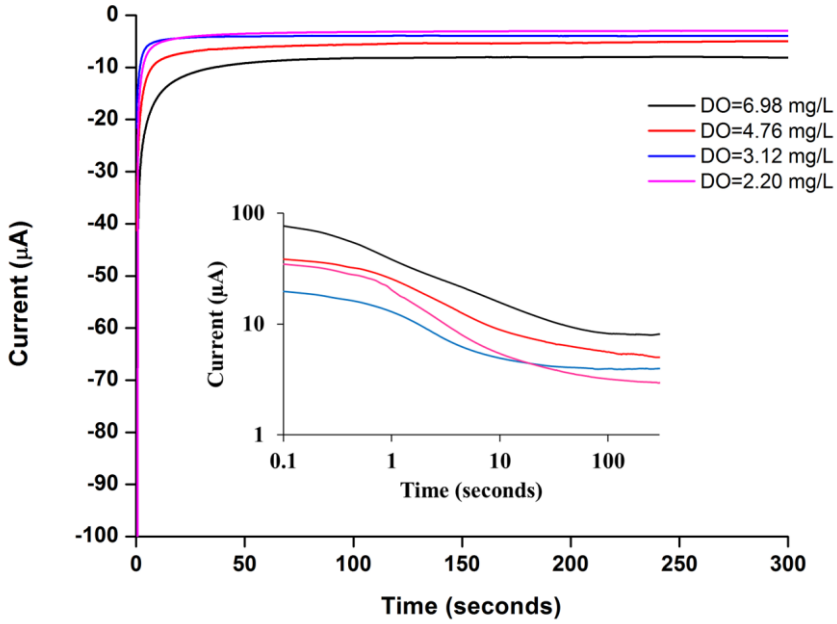

Figure 23 Current vs time graph from chronoamperometric measurements of Hemin based DO sensor (same graph represented in log-log scale in the inset figure). The different curves show the response from the sensors with water samples of different DO (dissolved oxygen) content values

3.6.2 Sensitivity calculation

The stable current values were plotted against the corresponding DO value of the water sample measured using commercial DO sensor. The slope of the line in the current vs DO gives the value of the sensitivity of the DO sensor in µA/mg/L. Figure 24 shows the current vs DO plot used to calculate the sensitivity.

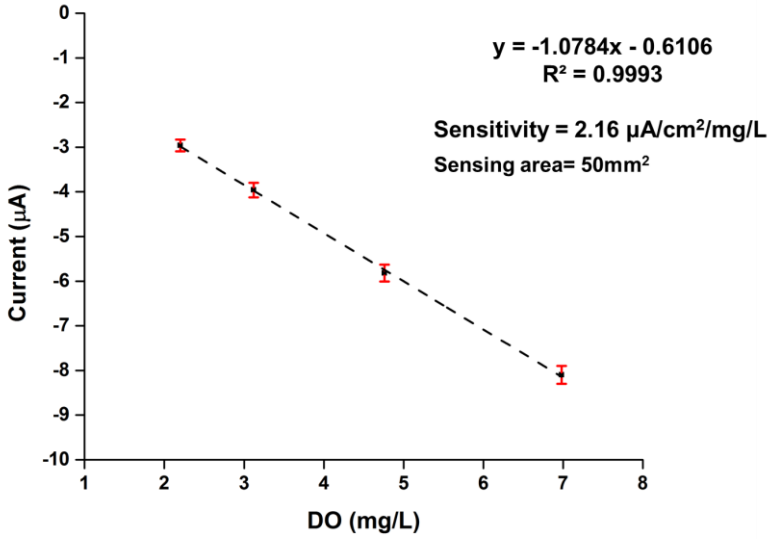

Figure 24 Current vs DO graph for hemin based DO sensors. The slope of the graphs gives the value of sensitivity of the sensor in µA/mg/L. Error bars are considerably smaller and represent standard deviation (SD)

3.7 Summary

In this chapter, the working concept, fabrication of device, experimental set and the methodology for the experiment and measurements is described. Based on the objective of this study, design criteria have been listed, and the device and experiments were designed accordingly. Membrane filtration in the tangential flow configuration is utilized to remove the solid and biological matter with the help of a flat ultrafiltration membrane. A customized tangential flow filtration (TFF) device is fabricated from acrylic (Poly methyl methacrylate) with the help of laser cutting and machining. Slots

were made in the bottom part of the TFF device by machining, for placing the microfabricated pH and dissolved oxygen (DO) sensors on the permeate side of the filtration device. A flat sheet of ultrafiltration membrane was used as membrane for the TFF device. Measurement set up for both the pH and DO sensors is explained.

The fabricated device was designed to remove the solid and biological matter from the water sample without changing its ionic composition and provide it to the sensors for reliable water quality monitoring for longer period of time. The next chapter describes the results obtained from the experiments performed in this study.

Chapter 4

Results and Discussion

In last chapter, the working concept of the TFF (tangential flow filtration) device, its design, fabrication, and the experimental setup to prevent biofouling on water monitoring sensors were explained in detail. This chapter presents the results from the experiments performed using the TFF device to prevent biofouling on microfabricated pH and DO (dissolved oxygen). Low cost, advanced, microfabricated pH and DO sensors were integrated in a customized TFF device and placed on the permeate side of the filtration device. A flat sheet ultrafiltration PES membrane was used as the filtration membrane in the TFF device. The sensors were subjected to tests with different samples and under different conditions. The results are represented as variation in signal and sensitivity for the sensors over a period of one week for all the conditions. The TFF device is shown to successfully control the degradation of the sensor performance in the accelerated biofouling conditions by filtering out the biological matter and preventing the formation of biofilm on the surface of the sensors. Further, an attempt was made for membrane fouling mitigation in the TFF device by comparing different spacer designs. humic acid (major component of natural organic matter) was used as feed for

visualization of membrane fouling for this experiment and image analysis was performed to compare the results from the different spacers.

4.1 Effect of accelerated biofouling on Pd/PdO based pH sensor and its integration with TFF device

In this section, the effect of accelerated biofouling on microfabricated Pd/PdO based pH sensor is presented. First, a control experiment is carried out without the TFF device and open circuit potential measurements are performed for the pH sensors kept in four different samples. Next, the sensor is integrated in the TFF device with accelerated biofouling solution as the feed. Open circuit potential measurements are presented and the results are discussed.

4.1.1 Effect of accelerated biofouling on Pd/PdO based pH sensor

The objective of this experiment was to demonstrate the effect of accelerated biofouling conditions on the microfabricated Pd/PdO pH sensor used in the study.

The pH sensors were kept in four different solutions in the control experiment. For the control experiment, TFF device was not used and the sensors were kept in four different samples in static condition (no flow of sample over sensor). In normal drinking water and natural surface water samples it would take longer time for the micro-organisms to grow. To accelerate this process, nutrients were increased by adding 1%

yeast extract to 1L tap water in order to prepare an accelerated biofouling solution. The samples used in the experiment were- an accelerated biofouling solution, 10mg/L humic acid, tap water and DI water. The accelerated biofouling solution was prepared by adding 1gm of yeast extract (Product Number: Y1625, Sigma-Aldrich, St. Louis, Missouri) to 100 mL tap water to prepare 1% w/v yeast extract solution [109]. Yeast extract is water soluble part of autolyzed yeast and is a mixture of amino acids, water soluble vitamins and carbohydrates. It acts as a source of nutrients for the microbes. The humic acid solution was prepared by adding 10mg humic acid (Product Number: 53680, Sigma-Aldrich, St. Louis, Missouri) in 1000mL DI water [100]. Humic acid is a major component of natural organic matter (NOM) and is present in all surface water bodies [110] [111]. It is often used for experiments in the laboratory, as a representative component of the natural organic matter from the natural surface water [112]. In this experiment, it was included as one of the samples in the control experiment to study its effect on the sensors' performance over time.

The sensors were placed in four solution samples in static condition and open circuit potential measurements were taken over a period of one week. With the help of a syringe, 10mL of air was bubbled every day in the accelerated biofouling solution for the growth of biological matter. The bubbled air provides oxygen in the solution which is required for the growth of microorganisms and is consumed from the solution in the

process over time. The sensors were taken out of the sample and were left to dry before carrying out the measurements.

Open circuit potential measurements were performed for the pH sensors at the beginning of the experiment and after the first, third, fifth and seventh day. The procedure for the measurements is described in the section 3.5.1. The open circuit potential of the sensor immersed in buffer solutions of pH= 4,6,7,8, and 10 were recorded. Palladium oxide has reversible reactions with hydrogen ions which results in the exchange of ions between the electrode and the solution containing hydrogen ions [113]. Due to the change of Gibbs free energy of this electrochemical system, the electrical potential at the electrode changes with the change in hydrogen ion concentration. Hence, the open circuit potential between the electrode and a reference electrode (Ag/AgCl in this case) is a function of the concentration of hydrogen ions [20]. In other words, the open circuit potential is a measure of the pH of the solution.

The open circuit measurement was followed by the calibration of the sensor with buffer solutions of pH values = 4,6,7,8, &10. The pH sensitivity of the sensors was calculated using the open circuit potential measurements for different pH buffers. The pH sensitivity values were then plotted against time to analyze the trend.

The results for this experiment are presented in the following graph.

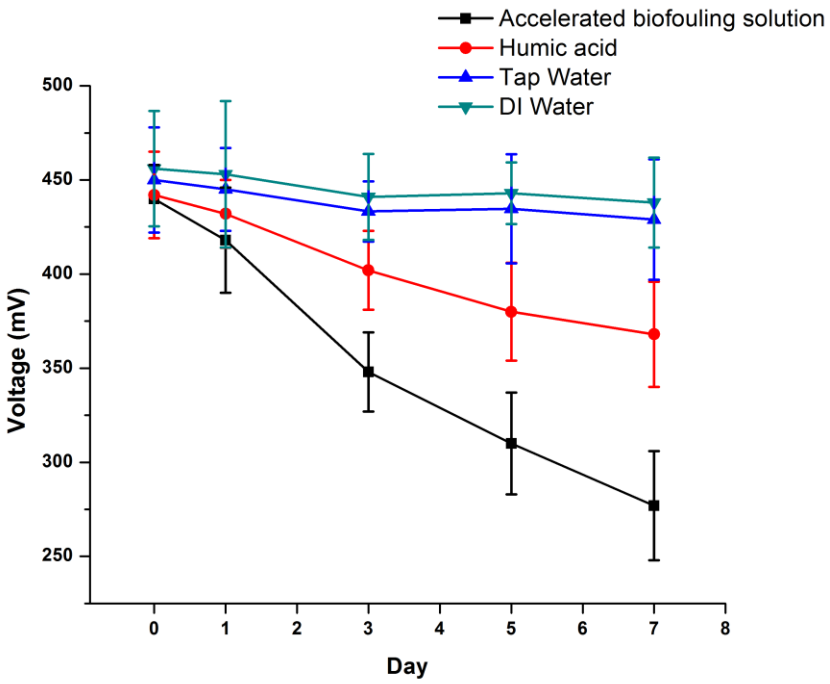

Figure 25 Response of the pH sensors kept in four different samples a) DI water, b) tap water, c) 10mg/L Humic acid and d) 1% yeast extract as accelerated biofouling solution from the open circuit potential measurement with buffer solution of pH=7. Error bars represent standard deviation (SD)

Figure 25 shows the change in the open circuit potential response of the pH sensors when placed in a test solution (buffer of pH=7) over a period of one week.

The open circuit potential for the sensors kept in DI water decreased from 456mV to 438mV, a ~4% decrease, over the time period of the experiment. For the sensors placed in tap water and humic acid, the decrease was ~3.7% and 16%, respectively. No significant change ($p=0.088$, $\alpha=0.01$, *where* α is the significance level in the statistical

analysis and *p-value* is the probability of obtaining a result equal to more than what was observed, when the null hypothesis is true) is observed in response observed from the sensors kept in tap water and DI water. However, the decrease in the open circuit potential for the sensors kept in accelerated biofouling solution was 37%, which is much higher than the decrease noted in the other 3 samples. The decline in the open circuit potential continues over the entire period of one week for the sensors.

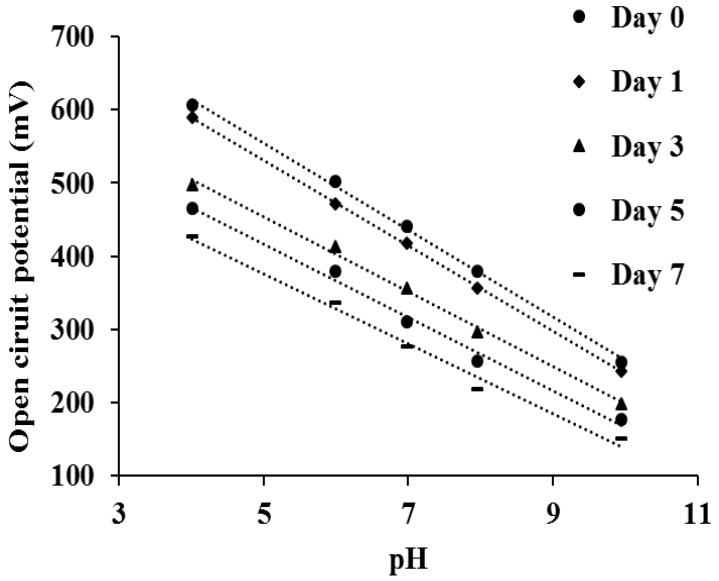

Figure 26 Open circuit potential (mV) vs pH for the sensors kept in accelerated biofouling solution

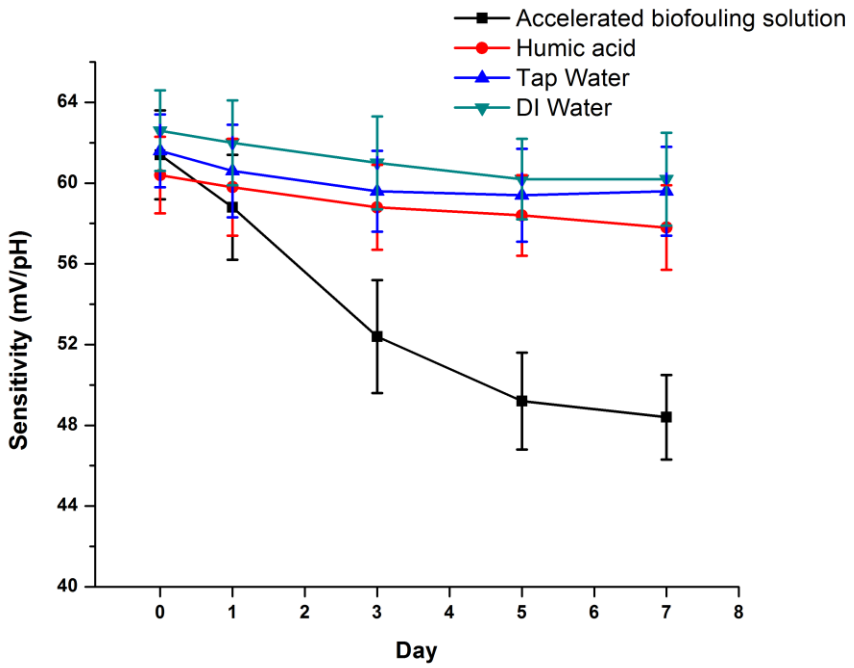

Figure 27 Changes in the sensitivity values of the Pd/PdO based pH sensors over one week when placed under static condition in four different solutions -a) DI water, b) tap water, c) 2mg/L Humic acid and d) 1% yeast extract as accelerated biofouling solution (inset figure shows OCP vs pH for sensor in acc. biofouling solution on different days). Error bars represent standard deviation (SD)

Figure 27 shows the change in the sensitivity of the sensors over the time period of one week. The pH sensors kept in tap showed a decrease in sensitivity from 61.6mV/pH to 59.6mV/pH over a period of 7 days, which is a decrease of ~3.2% in sensitivity. Similarly, the sensors kept in DI water and humic acid showed a decrease of ~3.0% and ~5.3% respectively. The sensitivity of the sensors stored in tap water

corresponds to a degradation rate of -0.28mV/pH/day (negative symbol denoting decrease in the value). In another study based on the same pH sensor, a degradation rate of -0.13mV/pH/day was noted when the sensors were used for a period of 60 days, while they were stored in ambient air for storage stability [20].

However, the sensitivity of the sensors kept in accelerated biofouling solution decreased from 61.4mV/pH to 48.4mv/pH, a loss of ~21%. It can be seen that the decrease in the sensitivity with time occurs rapidly in the first three days which is followed by gradual decrease after the third day.

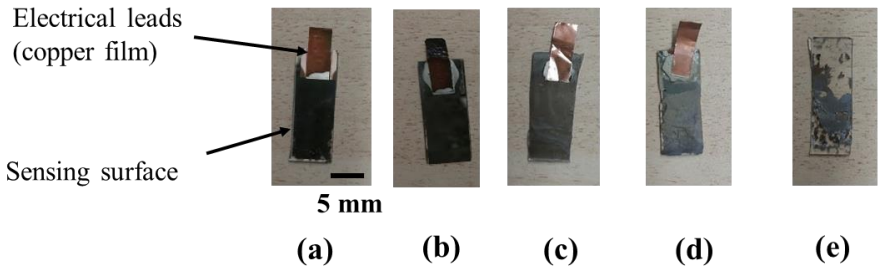

Figure 28 (a) pH sensor kept in DI water (b) pH sensor kept in tap water (c) pH sensor kept in 10mg/L humic acid (d) pH sensor kept in 1% yeast extract solution (e) pH sensor after 2 weeks of storage in accelerated biofouling solution

Figure 28 shows the pH sensors kept in different samples. It is observed that by the end of this time period of one week, the electrode layer on the glass substrate starts to form wrinkles on the surface. The formation of the wrinkles is followed by the peeling-off of the electrode from the glass substrate in the subsequent days, as seen in Figure 27(e). The peeling-off of the electrode from the sensors was observed to be much more aggressive for the sensors kept in the accelerated biofouling solution and the measurements were not feasible on the days after the first week due to poor contact between the electrode layer and the connectors. In case of the sensors kept in the other three solutions, the peeling-off was minimal. However, the wrinkles on the surface of the sensors were observed in the other three solutions as well.

Following observations are drawn from this experiment-

1) The sensitivity of the pH sensors declines significantly in accelerated biofouling condition as compared to when it is stored in DI water, tap water and humic acid. The decline in sensitivity value in accelerated biofouling conditions can be attributed to adhesion and subsequent growth of the microbes on the sensors surface. Images of the sensors were taken and analyzed under the microscope. The growth of the biofilm was observed on the sensor surface over the duration of the experiment. Similar trend in results indicating the decrease in the sensitivity due to biofouling has been observed in a study done on glucose biosensors [114].

2) The rapid decrease in the sensitivity value of the sensor in accelerated biofouling solution in the first three days can be explained by formation of a layer of nutrients on the sensor surface and the subsequent immobilization and exponential growth of the microbes in the initial phase. This can cause interference with the transfer of ions with the sensor surface for sensing.
3) There is no significant decrease in the sensitivity of the sensors kept in DI and tap water ($P=0.088,\ \alpha=0.01$). This indicates that the sensors performance does not vary for the DI and tap water over time and gives reliable long term measurements in the absence of accelerated biofouling environment. There is a small decline observed for the sensors placed in humic acid solution well. This decline could be due to the interference because of deposition of a thin layer of organic particulates dispersed on the sensor surface as observed under the microscope.
4) Observation from the results for the sensors kept in accelerated biofouling solution- Figure 25, displaying OCP (open circuit potential) at pH=7 vs days, shows that the absolute value of OCP continued to decline over the duration of the experiment. While, Figure 26 shows the decline in the sensitivity (which is the slope of the line in OCP vs pH graph for pH values from 4 to 10) was gradual towards the end of the experiment. As observed in the inset figure (in Figure 26), which shows the OCP (at

pH=7) vs pH for the sensors in accelerated biofouling solution for different days, the decline in the absolute OCP value is different from the change in the slope of the line.

This experiment shows that the open circuit potential measurement from the microfabricated Pd/PdO and its sensitivity decreases considerably over time in accelerated biofouling conditions.

The next step is the integration of the sensors with a tangential flow filtration device as an antifouling strategy.

4.1.2 Integration of pH sensor with TFF device as an antifouling strategy

The purpose of this experiment was to study the effect of accelerated biofouling solution on the microfabricated pH sensors after integrating them with a TFF device while placing the sensors on the permeate side of the filtration device such that only the permeate flows over the sensors.

In this experiment, the pH sensors were placed on the permeate side of the TFF device as described in Section 5.3.3. The feed used was 1% Yeast extract solution, an accelerated biofouling solution. The TFF device was operated with a feed flow rate of 150mL/min at a trans membrane pressure of 5 psi. This corresponds to a tangential velocity of 12.5cm/s. The TFF was operated for a period of 7 days and the open circuit potential for the pH after 1, 3, 5 and 7 days. The results from this experiment are presented as following.

To improve the longevity of the TFF device different flow conditions were considered. In this study two modes of operation were studied- continuous mode and intermittent mode. The different modes of operation were selected to examine and compare the results between the periodic and continuous modes of TFF operation. In continuous mode, the peristaltic pump is run continuously for the complete duration of the experiment. In this case, the filtration occurs throughout the experiment and the permeate passes over the sensor surface through the entire duration. In the intermittent mode, the peristaltic pump is run intermittently for 60 minutes every day just before taking measurements. During this time the filtration takes place and the feed (accelerated biofouling solution) flows over the membrane and the permeate passes over the sensor surface. For the remaining time, the peristaltic pump is kept off. During this time, the no filtration takes place. The chamber in which the sensors were placed remains filled with the permeate solution during this time and the surface of the sensors were in contact with the permeate.

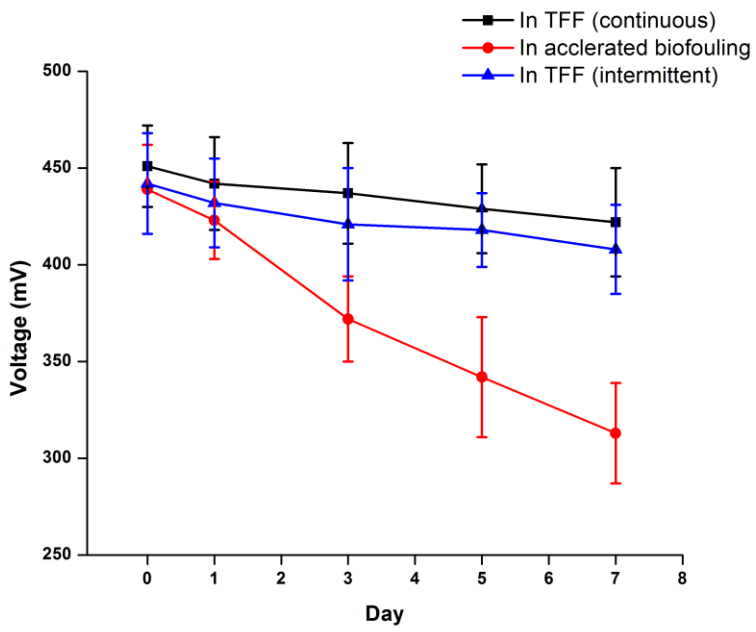

Figure 29 Response of the pH sensors integrated in TFF device with the buffer solution of pH=7. Error bars represent standard deviation (SD)

Figure 29 shows the change in response of the sensors in the open circuit potential measurements with the buffer solution of pH=7. The open circuit potential for the pH sensors integrated with the TFF in continuous mode decrease from 451mV/pH to 422mV/pH, a decrease of ~6%. A similar decrease of ~7.7% in sensitivity is observed in the sensor integrated with the TFF in intermittent mode. However, in the accelerated biofouling conditions, the open circuit potential decreases significantly by ~28%

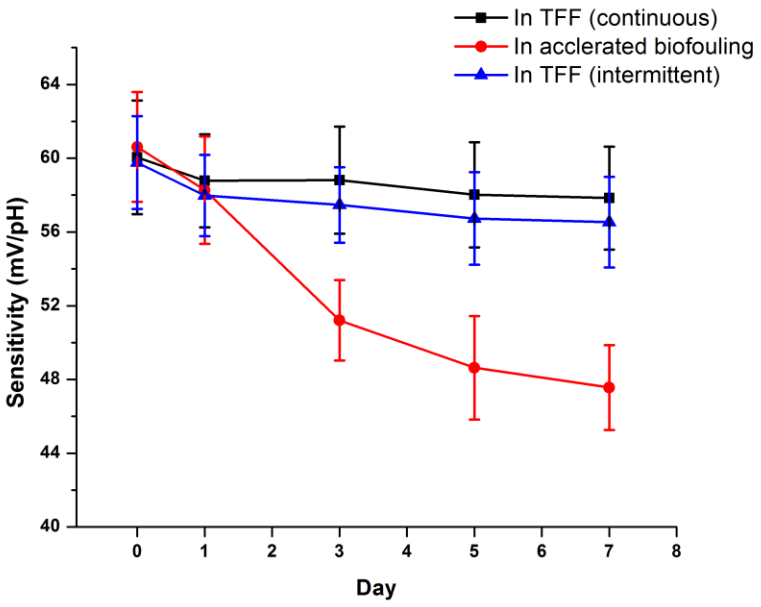

Figure 30 Change in the sensitivity values of the sensors over one week when kept in three different conditions- a) integrated with TFF device in continuous run b) in accelerated biofouling solution, and c) integrated with TFF device in intermittent mode. Error bars represent standard deviation (SD)

Figure 30 shows the change in the sensitivity of the sensors over the time period of one week. The decrease in the sensitivity of the sensor with the TFF device in continuous mode decreases from 60mV/pH to 57.8mV/pH, a decrease of ~4%. A similar decrease of ~6.4% in sensitivity is observed in the sensor integrated with the TFF in intermittent mode. This is different from the case when the sensor is not integrated with the TFF and a significant decrease of ~21% in the sensitivity is observed over the period of 7 days.

A gradual decreasing trend is observed for both the continuous and intermittent mode of operation of TFF. Whereas the decrease in the sensitivity occurs rapidly in the first three days for the sensors kept in accelerated biofouling solution.

Following observations can be made from this experiment-

1) As observed in the control experiment, the sensitivity of the pH sensors declines rapidly in the accelerated biofouling solution when the sensors were directly in contact with the biofouling solution. However, the decline in sensitivity is gradual when the sensors were integrated in the TFF device (placed on the permeate side of the filtration device). In this case, the accelerated biofouling solution gets first filtered through the ultrafiltration membrane before passing over the sensors surface. The pore size of the membrane is selected as 300kDa which is approximately 35nm [100]. This pore size is sufficient to remove most of the biological matter as well as bacteria. This can prevent the contact of the bacteria from the sensor surface and the formation of the biofilms on the surface of the sensors.
2) There was no significant difference in the sensitivity of the sensors integrated with TFF in the continuous and intermittent mode. In both the modes the deterioration of the sensor performance was much lesser as compared to when the sensors were directly in contact with the accelerated biofouling solution. This can be explained by the fact that the feed (accelerated biofouling solution) was filtered through the

ultrafiltration membrane in both the cases which contributed in preventing the biofouling on the sensor surface.

This experiment demonstrates that the integration of the pH sensors with the tangential flow filtration device is helpful in controlling the deterioration of the pH sensor performance in accelerated biofouling conditions.

4.2 Effect of accelerated biofouling on hemin based DO sensor and its integration with TFF as an antifouling strategy

In this section, the effect of accelerated biofouling on microfabricated hemin based DO sensor is presented. First, a control experiment is carried out without the TFF device and chronoamperometric measurements are performed for the DO sensors kept in four different samples. Next, the sensor is integrated in the TFF device with accelerated biofouling solution as the feed. Chronoamperometric measurements are presented and the results are discussed.

4.2.1 Effect of accelerated biofouling on hemin based DO sensor

The objective of this experiment was to demonstrate the effect of accelerated biofouling on the microfabricated hemin based DO sensor used in this study.

The DO sensors were immersed in four different solutions for the control experiment. For the control experiment TFF device was not used. The solutions used

were: accelerated biofouling solution (1% Yeast extract in tap water), 10mg/L humic acid, tap water and DI water. The sensors were taken out of the sample and were left to dry before carrying out the measurements. Chronoamperometric measurements were performed for the DO sensors at the beginning of the experiment and after the first, third, fifth and seventh day. The procedure for the measurements is described in section 3.6.1. The measurements for the stable current values from the sensors were noted for each of the sample water solutions for calibration. A commercial DO meter (550A dissolved oxygen meter, YSI Incorporated, Ohio) was used to measure the dissolved oxygen content of the water samples used for calibration. The DO values of the samples for calibration were obtained by purging Nitrogen gas (to decrease DO levels) and Oxygen gas (to increase DO levels) to tap water samples. The sensitivities of the sensors were calculated using the current value measurements and plotted against time to analyze the trend.

The results for this experiment are presented as below.

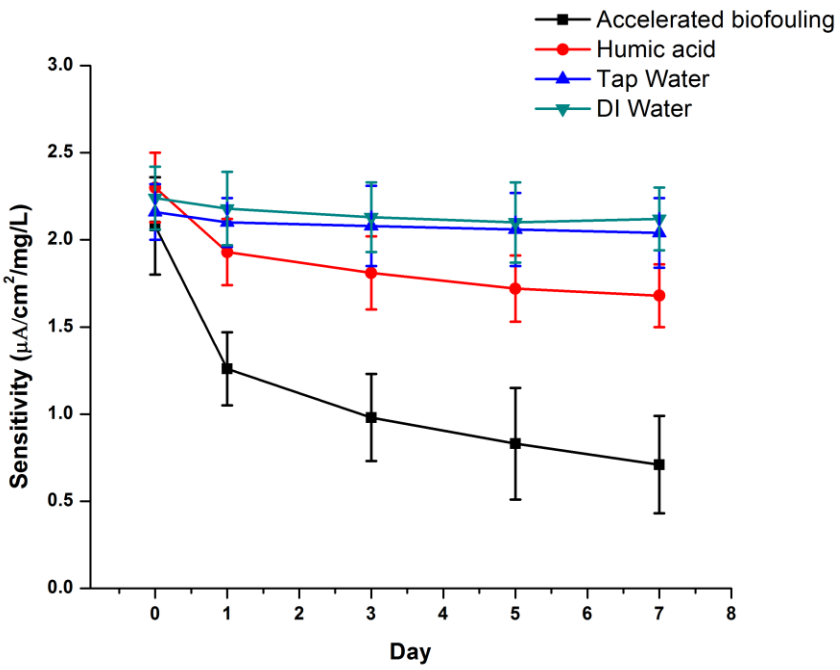

Figure 31 Change in the sensitivity values of the DO sensors placed in four different solutions- a) DI water, b) tap water, c) 10mg/L Humic acid and d) 1% yeast extract as accelerated biofouling solution. Error bars represent standard deviation (SD)

Figure 31 shows the change in the sensitivity of the DO sensors over the time period of one week. The sensitivity of the DO sensors kept in DI water decreased from 2.14 µA/cm^2/mg/L to 2.12 µA/cm^2/mg/L, a decrease of ~5% in sensitivity over a period of 7 days. The decrease in the sensitivity value for sensors kept in tap water and humic acid solution was ~6% and ~25%, respectively. However, the decrease in the sensitivity for the DO sensor kept in accelerating biofouling solution was ~66%. In a similar study

on this DO sensors, a decrease of ~67% was observed when the sensors were subjected to accelerated biofouling conditions [108].

It can be seen in the graph that the decline in the sensitivity for the sensors kept in accelerated biofouling solution and the humic acid solution occurs rapidly in the in first few days and decrease gradually slows down after that. For the sensors kept in the DI water and tap water, the decline is significantly slow.

Following observations can be made from this experiment-

1) The sensitivity of the DO sensors decreases significantly (66%) in the accelerated biofouling solution as compared to DI water and tap water. This again, can be explained by the immobilization and the subsequent growth of bacteria on the sensor surface when it is subjected to the accelerated biofouling solution. The biofilm layer can act as barrier to the diffusion of oxygen and effect the sensor's performance. This result is similar to another study carried out on the same sensor in which a
2) The decrease in the sensitivity of the DO sensors (66%) in accelerated biofouling solution is much more than the decrease of the sensitivity of the pH sensors (21%). Also, there is a smaller decrease in the sensitivity of the DO sensors placed in humic acid as compared to the sensors placed in accelerated biofouling solution. This can be explained by the difference in the properties of the top layer of the sensors. The top layer of DO sensor is PDMS (Polydimethylsiloxane) which is inherently prone to

biofouling due to it hydrophobic nature. Due to this, the biological matter can easily adhere to the sensor surface and the effect of biofouling is more predominant in the DO sensor. The decrease of 25% in sensitivity value of the DO sensor in humic acid can also be explained due to this.

This experiment shows that the hemin-based DO sensors deteriorates and loses its sensitivity over time in accelerated biofouling conditions.

4.2.2 Integration of DO sensor with TFF device as an antifouling strategy

The purpose of this experiment was to study the effect of accelerated biofouling solution on the microfabricated DO sensors after integrating them with a TFF device while placing the sensors on the permeate side of the filtration device such that only the permeate flows over the sensors.

In this experiment, the DO sensors were placed on the permeate side of the TFF device as described in Section 3.3.4. The feed used was 1% Yeast extract solution, an accelerated biofouling solution. The TFF device was operated with a feed flow rate of 150mL/min at a trans membrane pressure of 5 psi. This corresponds to a tangential velocity of 12.5cm/s. The TFF was operated for a period of 7 days and the open circuit potential for the pH after 1, 3, 5 and 7 days. As described in section 4.1.2, the TFF device is operated in two modes- continuous and intermittent. The results from this experiment are presented as following.

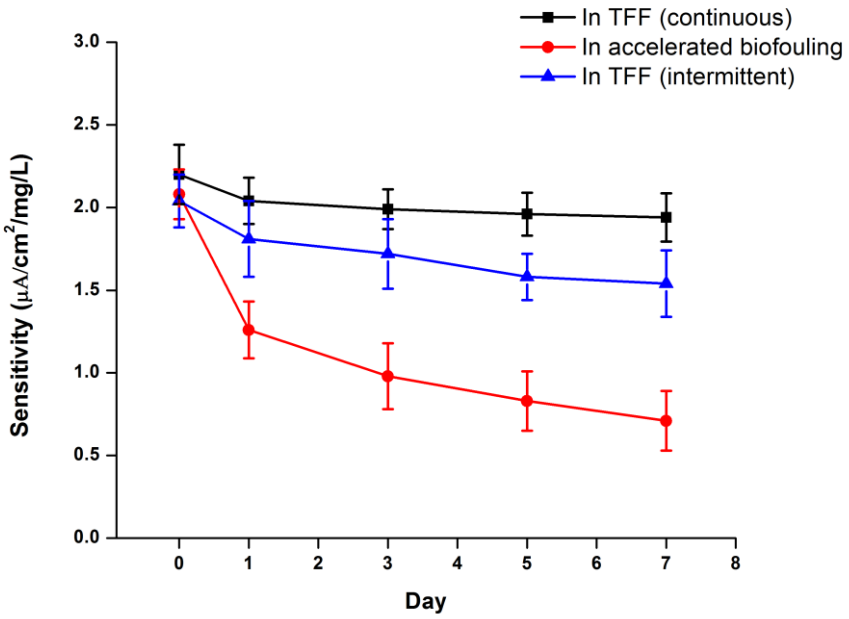

Figure 32 Change in the sensitivity values of the DO sensors integrated in TFF device. Error bars represent standard deviation (SD)

Figure 32 shows the change in the sensitivity of the sensors over the time period of one week. The decrease in the sensitivity of the sensor with the TFF device in continuous mode decreases from 2.14 µA/cm^2/mg/L to 1.94 µA/cm^2/mg/L, a decrease of ~10%. A similar decrease of ~24% in sensitivity is observed in the sensor integrated with the TFF in intermittent mode. This is different from the case when the sensor is not integrated with the TFF and a significant decrease of ~66% in the sensitivity is observed over the period of 7 days.

The decrease in the sensitivity occurs rapidly in the first three days for the sensors in all conditions which is followed by gradual decrease for the remaining time period.

Following observations can be made from this experiment-

1) There is a significant loss of sensitivity of the DO sensor (~66%) in the accelerated biofouling conditions as observed in the control experiment. However, when the sensor is integrated with the TFF device and placed on the permeate side of the filtration device the loss of sensitivity is much lesser (~10%). This can be explained by the use of an ultrafiltration membrane which filter out the microbes from the feed and prevents the contact of the microbes from the sensor surface. This helps in preventing biofilm on the sensor surface which interferes with the diffusion of oxygen.
2) Comparing the results between these two modes, it can be observed that there is ~12% decline in the sensitivity value in the continuous run and a ~24% decline in the sensitivity value in the intermittent mode of filtration. This may be attributed to the hydrophobicity of the top PDMS layer which might get affected by the nutrients that pass through the membrane and remain stagnant for extended duration.

This experiment demonstrates that the integration of the DO sensors with the tangential flow filtration device is helpful in controlling the deterioration of the DO sensor performance in accelerated biofouling conditions.

4.3 Feed and permeate analysis

In this section shows the difference between feed and the permeate from the TFF device after filtration of the accelerated biofouling solution is analyzed. The feed solution when passed through the Tangential flow filtration device splits into two stream- permeate and retentate as shown in schematic in the Figure 18a.

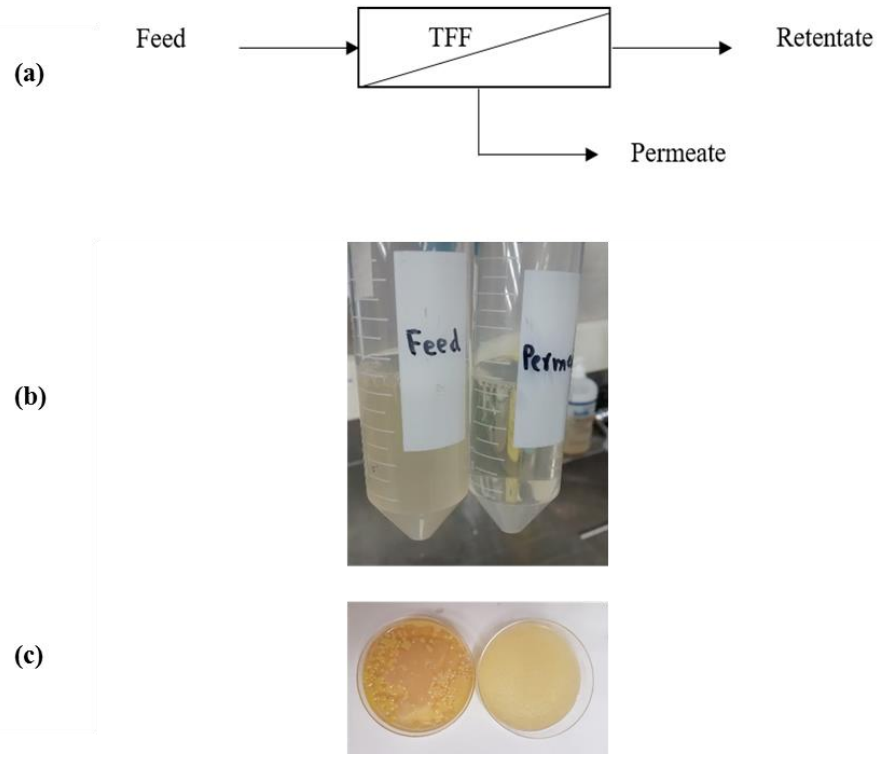

Figure 33 (a) Schematic of TFF showing the streams (b) Feed sample on left and Permeate sample on the right (c) Feed sample (left) and permeate sample (right) cultured on agar plate

Figure 33a shows the feed and the permeate solution after the duration of the experiment. As seen in the figure, the feed sample has a cloudy appearance while the permeate sample is relatively transparent. To check for the presence of biological matter, the feed and the permeate samples were collected after the measurement and cultured on agar plate. The procedure involves serially diluting the samples in a bio-safety cabinet and spreading 100µl of serially diluted sample on nutrient-rich agar plate. The agar plates were then stored at 37°C in an incubator for 24 hours. This leads to the growth of the biological matter present in the sample, if any. It can be seen in Figure 33b, there is biological growth observed in the feed sample plates and no such growth is observed on the permeate sample plates. The results indicate that biological matter is filtered out from the accelerated biofouling solution and the permeate likely does not contain biological matter that adheres to the sensor surface and cause biofouling of the sensors.

4.4 Permeate flux and Membrane Fouling

The major obstacle for any application of membrane processes is the decline of the permeate flux over time as a result of membrane fouling [34]. In this section, the permeate flux variation is noted over the duration of the experiment and different spacers designs are studied to achieve enhanced permeate flux as compared to the conventional flat channel spacer.

In the current study, the TFF device is operated at constant pressure with a feed flux of 150 mL/min at a trans membrane pressure of 5 psi. This corresponds to a crossflow velocity of 12.5cm/s in the channel. The spacer used inside the filtration device in this experiment was a conventional spacer with a flat channel having a rectangular cross section. The channel has a height of 1mm and width 20mm. The length of the channel is 100mm. The permeate is collected in a conical flask and the mass of the collected permeate is measured using Ohaus Scout Pro Portable Electronic Balance (Part no. SP6000). The data is continuously collected on a computer to calculate the permeate flux. At the outset, the permeate flux is calculated after 30 minutes of starting the experiment to reach a stable permeate flux. Thereafter, permeate flux is noted after every 24 hours to study the flux variation over the duration of the experiment.

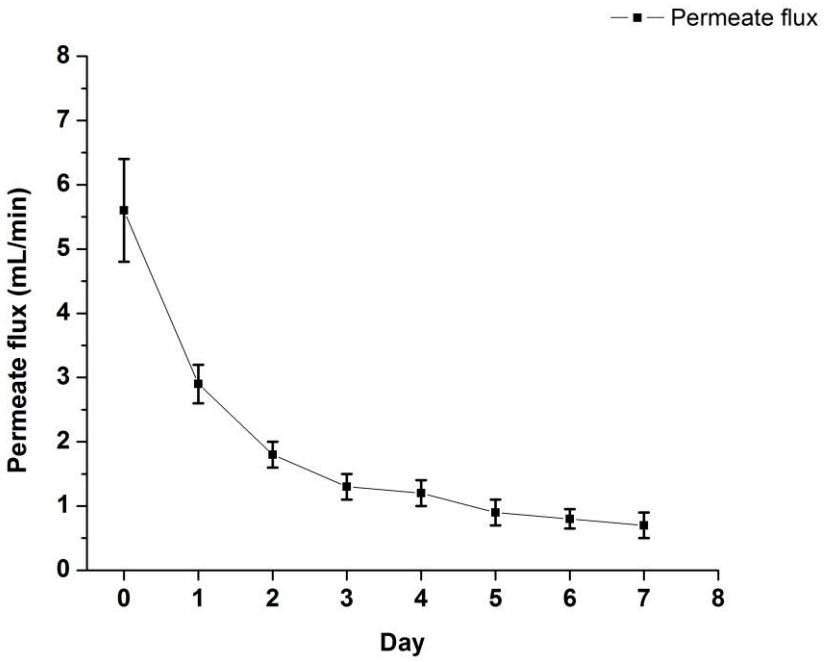

Figure 34 Permeate flux variation over the duration of the experiment using the Tangential Flow Filtration device with accelerated biofouling solution as the feed sample

As represented in Figure 34 the permeate flux decreases over the duration of this experiment. There a significant decrease in the first day and towards the end of the experiment the flux reduces from 5.6 ± 0.8mL/min at the beginning to 0.7 ± 0.2mL/min, a decrease of ~88%. The loss in the permeate flux is undesirable in membrane filtration processes. Even though it is not completely avoidable, several methods have been used to control the amount of fouling on the membrane. In this study, an attempt has been made to control the fouling of the membrane by using a passive hydrodynamic method which

involves using spacers with grooves to enhance the permeate flux. The following section describes the different spacers used and the results obtained with the spacers.

4.4.1 Spacer design and image analysis of membrane fouling

Spacers with different groove designs were used in this study to compare the effect on the humic acid fouling on the ultrafiltration membrane. These spacers were cut on 0.5mm acrylic sheet using laser cutting and used in the TFF device to compare the fouling on the PES ultrafiltration membrane of pore size 300kDa.

The spacer designs as shown in Figure 35 have been used in this study to compare the results with the conventional flat channel rectangular cross-section spacer. Four different spacers were used with different groove shapes. Figure 35a shows the conventional flat channel. The spacer with rectangular grooves is shown in Figure 35b. Saw-toothed, sinusoidal, spacer and woven fiber structures have been earlier used to increase the permeate flux in tangential flow filtration by means of increasing the shear stress on the membrane [115] [116] [117] [118]. The filtration enhancement mechanism is attributed to the intensification of the flow field near the membrane surface [115] [116]. Due to this, higher shear rates are developed in the thinner flow boundary layer which produce stronger scouring force for the deposited particles or solute and helps in reducing fouling [115]. However, these studies have been tested for high flow rates and high Reynolds number, typically $800<Re<1850$. In this thesis, staggered herringbone

channels were used to study its effect on the membrane fouling using image analysis. These spacers are as shown in Figure 35 c,d,e with three, two and one number of grooves (n=3,2,1). These structures have been earlier used, mainly in microfluidics to produce enhanced mixing at low Reynolds number [119]. The staggered herringbone grooves were used to induce mixing in the channels at very low Reynolds number, typically $0 < Re < 100$. These have been described as micro vortex-generating structures that help in generating vortex by passive means and have been implemented for enhancing the capture of certain cells on the channel walls with the help of increased mixing in the channel[120]. These have also been shown to enhance the performance of biosensors by increasing the mass transfer [121] [122] [123]. In this study, these spacers were used to study the effect on membrane fouling and compare the results with the conventional flat channel spacers.

The feed used in this experiment is 10ppm humic acid solution. Humic acid is generally used for studying membrane fouling as it a major component of natural organic matter and is present in all surface waters. The experimental apparatus is explained in Section 3.8. The experiment is carried out for a duration of 90 minutes with a feed flow rate of 300mL/min at a trans membrane pressure of 10psi. Higher trans membrane pressure condition was used to shorten the duration of the experiment for membrane fouling.

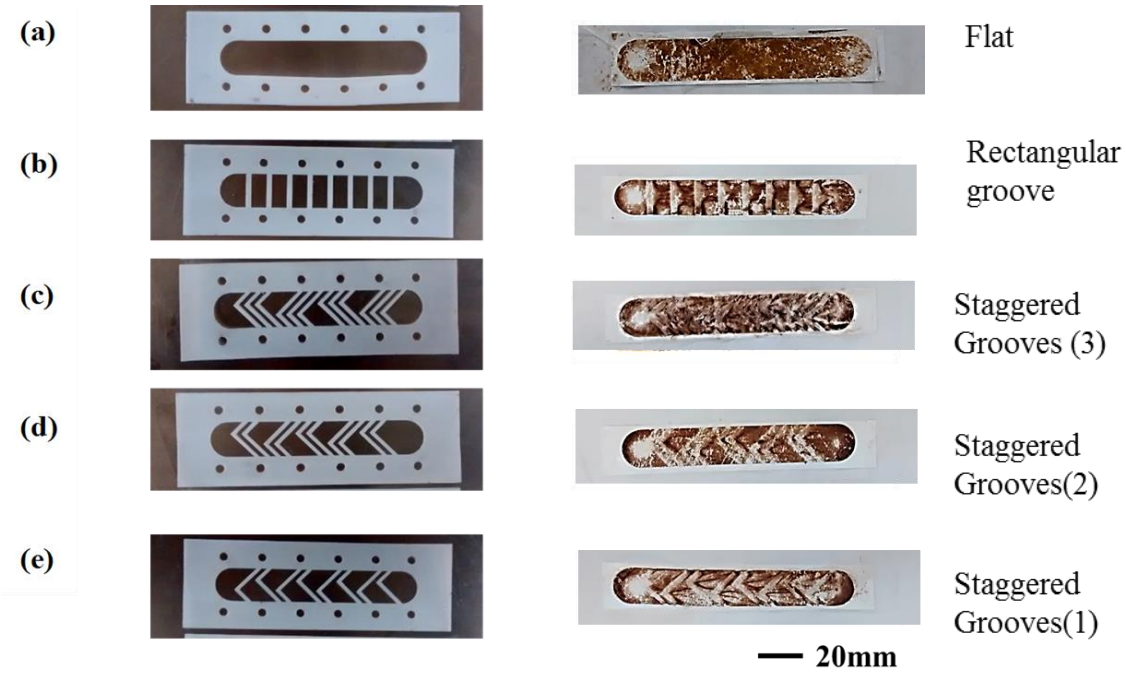

Figure 35 (a) Flat channel spacer (left) and the respective fouled membrane (right) (b) Rectangular grooved channel (left) and the respective fouled membrane (c) Staggered herringbone grooved spacer (left) with n=3 in (c), n=2 in (d) and n=1 in (e) and the respective fouled membranes (right)

Image analysis was performed for the fouled membranes using ImageJ software (Appendix A). The results are presented as below.

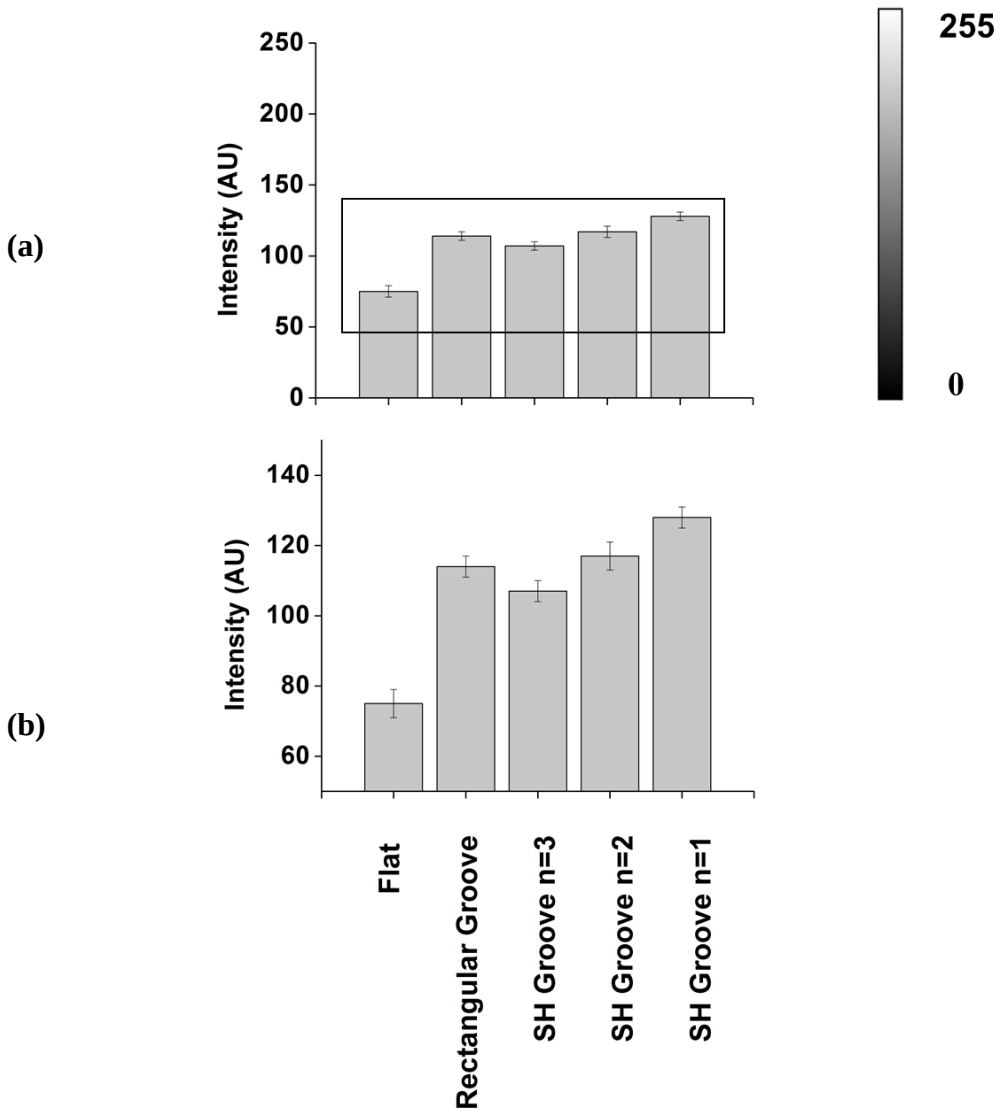

Figure 36 (a) Comparison of Intensity of the fouled membranes used in TFF device with different spacers (b) Zoomed in image of the area marked in Fig (a). On the y-axis, the intensity values vary within the range 0-255, with 255 denoting absolute white image.

Figure 36 shows the intensity values obtained after the image analysis of the fouled membrane images. Following observations are made from the image analysis-

1. The fouling in the flat channel is observed to be more than all the grooved spacers and is spread uniformly across the membrane.
2. There are patterns observed in the grooved spacers and the fouling is more at some areas. In the asymmetric grooves spacers, there is lesser overall fouling. This is attributed to the flow instabilities induces by the staggered herringbone grooves and the increase in overall shear rate (Appendix B).

The channel with the least extent of fouling using humic acid is then used in the TFF device and permeate flux is measured for a period of one week to compare the results. This is discussed in the following section.

4.4.2 Permeate flux for grooved spacer

The objective of this experiment was to compare the different shape of spacers to study the effect on the permeate flux. In this section the spacer with the least observed fouling from the image analysis was used in the TFF device to compare the permeate flux variation over the entire duration of the experiment.

In this experiment, the TFF device is operated at constant pressure with a feed flux of 150 mL/min at a trans membrane pressure of 5 psi. The feed is an accelerated biofouling solution (1% yeast extract solution). The experiment is carried out for a

duration of 7 days. The permeate flux is measured every day and is plotted against time to analyze the trend.

Figure 37 shows the permeate flux variation over the duration of one week for the flat and the grooved spacer. In both the cases, there is a significant decline in the permeate flux. For the flat spacer, the initial permeate flux was 5.6mL/min and the permeate flux after a period of 7 days was 0.8mL/min, corresponding to a decrease of 86%. The grooved spacer permeate flux decreased from an initial value of 7.2mL/min to 2.1mL/min, corresponding to a decreased of 71%.

The flux decreases rapidly in the first two days and gradually thereafter.

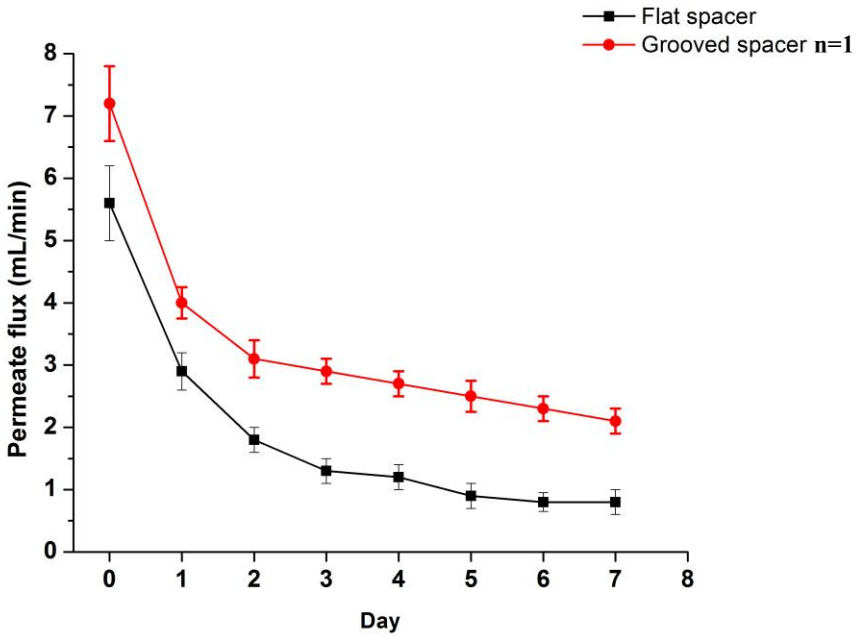

Figure 37 Comparison of permeate flux variation between flat and grooved channel

It is noted that the initial flux is higher for the grooved space with staggered herringbone grooves as compared to conventional flat channel. This can be attributed to the non-symmetricity in the channel and the higher shear flux in the channel due to the presence of grooves [124] [115]. The decrease in the permeate flux over the period of one week for grooved spacer configuration (~71%) is lesser than the decrease in the flat channel. Also, the higher flux is observed to be maintained over the time period of the experiment.

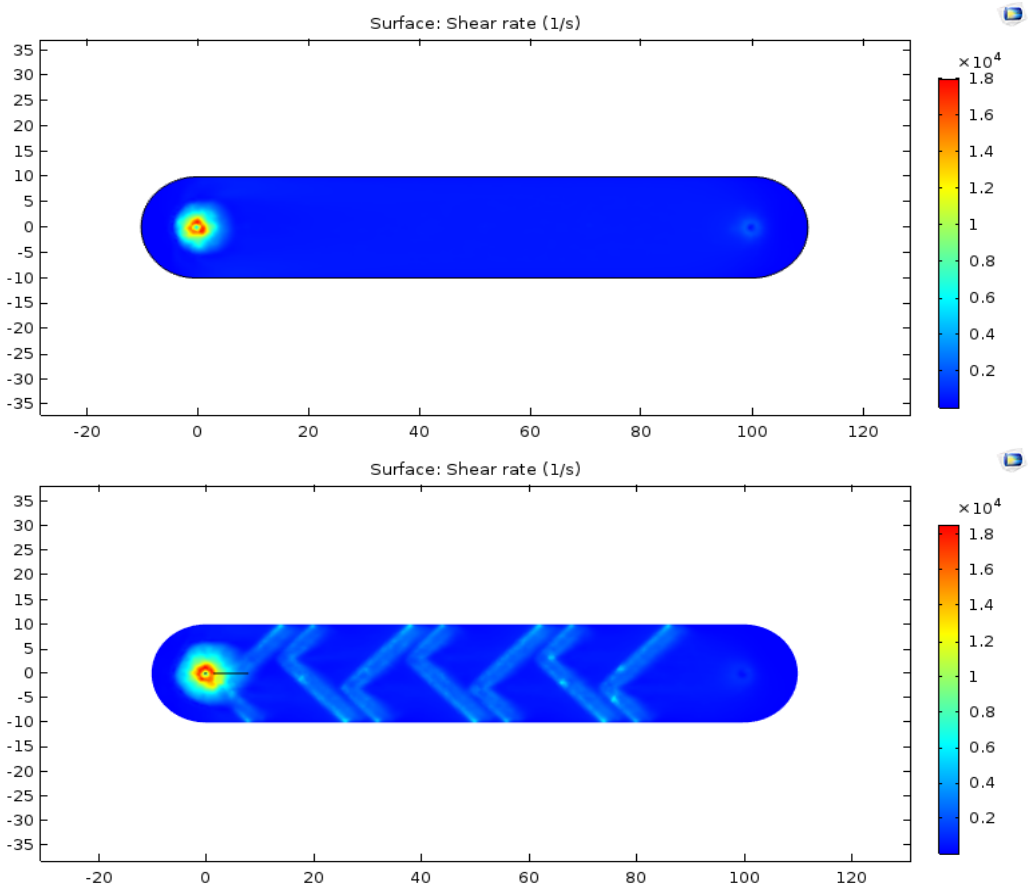

Figure 38 Shear rate distribution at the bottom surface of the flat channel (top) and the staggered grooved channel with n=1 (bottom)

The staggered herringbone grooves have been used in microfluidics for mixing fluids at low R_e numbers as passive mixing method [119]. In this study, the staggered herringbone grooved spacer was used to induce flow stabilities and increase the shear rate to increase the permeate flux. Figure 38 shows the shear rate distribution at the bottom surface of the flat channel (top) and the staggered grooved channel with n=1 (bottom) obtained with COMSOL® (appendix B). The results were mesh independent and the average shear rate for the grooved spacer was found to be 42% ($1388s^{-1}$as compared to $972s^{-1}$) higher than the flat channel spacer. The flow instabilities induced by the staggered herringbone grooves along with the increase in the average shear rate attributed to the increase in the permeate flux in the grooved spacer.

This experiment shows that the decline in the permeate flux is lesser for the grooved spacer as compared to the conventional flat spacer.

4.5 Summary

In this chapter, the effect of accelerated biofouling on the microfabricated pH and DO sensors was presented at the outset. The experimental results were illustrated with the help of response measurements from the sensors and the change in their sensitivity values over time. Thereafter, results from the sensors integrated in a Tangential Flow Filtration device (with a flat ultrafiltration membrane) were discussed. To study the membrane fouling in the filtration device, different spacer designs were used with humic acid

solution (major component of natural organic matter) as the feed. Image analysis of the fouled membranes was performed to compare the extent of fouling on the membrane.

The results from the experiments illustrate that the accelerated biofouling conditions lower the response from both pH and DO sensors within a few days of immersion. The integration of the sensors with the tangential flow filtration device while placing on the permeate side is shown to control the performance deterioration in accelerated biofouling environment for both the sensors. Image analysis and subsequent filtration experiments illustrates that the staggered herringbone grooved spacer was useful in maintaining a higher permeate flux as compared to the conventional spacer with rectangular cross section.

Chapter 5

Conclusion and Future Work

5.1 Contributions

The two main contributions of this thesis are- the integration of microfabricated pH and DO (dissolved oxygen) sensors with a customized tangential flow filtration (TFF) device to prevent the biofouling on the surface of the sensors and the use of grooved channel spacer in the TFF device to mitigate the fouling on membrane. These are described as following.

5.1.1 Integration of pH and DO sensors with TFF for preventing biofouling

As compared to the current antifouling methods described in Chapter 2, the use of a TFF module with ultrafiltration membrane is a cleaner method which requires minimum maintenance and can be easily used by unskilled personnel. It was noted from the from the experiments that the TFF device helped in the preventing the degradation of the sensitivity of both pH and DO sensors in accelerated biofouling conditions. When subjected to accelerated biofouling conditions, the sensitivity of pH sensors decreased by ~21% and the sensitivity of DO sensors decreased by ~66%, over a period of one week. However, when the sensors were integrated with the TFF device and placed on the

permeate side of the filter, the decrease for the pH and DO sensors was ~4% and ~10%, respectively. Following are the advantageous of using this method as an antifouling strategy as compared to the current antifouling methods-

1) Easy fabrication

The TFF device can be easily fabricated with the help of laser cutting and milling, and can be implemented in mass production with low cost per unit. The device is made from acrylic sheet which is relatively cheap. The other parts such as tubings and connectors are cheap as they are purchased in bulk.

2) Easy to operate and minimal maintenance

This method involves the insertion of an ultrafiltration membrane and sensors in the TFF module and assembly of the parts. It is an easy-to-operate device and can be used by unskilled personnel. The operation of the device requires minimum replacement and maintenance.

3) Clean technology

It is a clean technology and is environmentally safe. It does not produce any hazardous chemical waste that may affect the environment. The membrane process prevents the contact of the bacteria and solid organic matter from the sensor surface by physical separation of these from the feed. This method does not involve use of any

chemical or electric current in the feed (which may produce harmful species) and is easy to implement.

5.1.2 Improved spacer design for TFF module

It has been shown with the help of image analysis of the fouled membranes, that the grooved channel spacer maintains higher permeate flux as compared to the conventional flat channel spacer. The permeate flux decline over the period of the experiment for the grooved channel spacer was 71% as compared to 88% decline for the flat channel spacer. This shows that a modified spacer design can be beneficial in reducing membrane fouling.

5.2 Recommendations and future work

The preliminary experiments carried out in this study has shown that the tangential flow filtration device with an ultrafiltration membrane can prevent the biofouling on microfabricated pH & DO sensors and the grooved channel spacer gives higher permeate flux as compared to the conventional flat channel spacer. Nevertheless, more work need to be carried out including:

1) Development of the device for in situ measurements: To develop the device further for making it suitable for in situ measurements, the reference electrodes can be inserted along with the sensing electrodes in the slots made in the bottom part of the device. Also, an inlet and an outlet can be provided for injecting the buffer solutions

into and out of this slot. This would eliminate the need to disassemble the TFF device and to remove the sensors out of the TFF device for calibration.

2) The TFF device can be scaled down to a smaller size (by reducing the length and width of the channel) and can used with a peristaltic pump with lower flow rates. This would lower the associated costs due to reduction in the power requirement as well as reduction in the membrane area.
3) Testing with other sensors: The sensors used in this study were microfabricated pH and DO sensors. In future, the device can be tested for a wide range of sensors or devices that are highly susceptible to biofouling such as environmental sensors (for temperature, alkalinity, etc.) and biosensors which are predisposed to microbial biofouling.
4) Some of the water quality parameters such as dissolved oxygen is pressure-dependent and in this study, the feed sample was subjected to pressurized conditions inside the TFF device. Further study can be carried out to examine the effect of pressurized conditions (though not directly exposed to atmospheric oxygen) on DO measurement. In addition, an investigation of the effect of membrane fouling on the quality parameters (pH and DO) in the water samples (difference between feed and permeate) can be carried out.

5) In the current study, buffer solutions were used for measurements from the sensors. In future, the device can potentially be used in the field for drinking water samples and natural environmental water samples.
6) Finally, from the end users' perspective, the device can be operated on periodic basis as it was noted that the results from the continuous and intermittent modes were statistically insignificant. Moreover, periodic use would lead to less frequent replacement of the membrane and prolong the lifetime of the peristaltic pump.

5.3 Summary

In conclusion, the device developed for this thesis is a tangential flow filtration (TFF) device which is integrated with microfabricated pH and dissolved oxygen (DO) sensors to prevent biofouling on the sensor surface in accelerated biofouling conditions. Additionally, the grooved spacer used in the TFF device was shown to maintain higher permeate flux as compared to the conventional flat spacer when used with the accelerated biofouling solution as the feed. The device is easy to fabricate and requires minimal repair, maintenance, and replacement. It is a compact device that prevents biofouling on sensors surface and mitigates membrane fouling. It is mounted on a common platform with peristaltic pump to form an integrated system. Overall, it is a portable system and can be used for in-field water quality sensors. Finally, some recommendations are suggested for further development of the device.

Appendix A:

Image analysis using ImageJ

1. Open image file:

- Select ***File***, ***Open*** and upload the image file for processing. All the images of the fouled membrane used for analysis should be taken under the same lighting conditions.

2. Image type:

- From the menu bar, select ***Image, Type, 8-bit***. This saves the images in the type that can display 256 (2^8) gray levels (integers only). The digital images are two-dimensional grids of pixel intensities values with the height and width of the image defined by the number of pixels in rows and columns. Pixels (picture elements) are the smallest single components of images, holding numeric values that range between black and white.

3. Set the measurement scale

- Draw a line between 2 points with known distance on the image. Go to ***Analyze*** → ***Set Scale***. In the set scale window the length of the line will be displayed in pixels.

Enter the known distance and units of measure in the appropriate boxes and click OK.

4. Area selection

- From the area selection tool, select the ***rectangular*** shape option and surround the area of the fouled membrane.
- Go to ***Image, zoom*** and use ***In [+]*** to zoom in and fit the shape along the boundary of the fouled membrane area. The subsequent measurements are done for this enclosed membrane area, separating it from the rest of the image.

5. Measurements and analysis

- Go to ***Analyze → Set measurements*** and selected area, mean gray value and min and max gray value.
- Select ***Analyze → Measure*** to obtain the mean gray value as selected in the previous step. The mean gray value is noted and compared for the different fouled membranes.

Appendix B:

COMSOL simulation set up

1. Model Selection:

- Select ***3D*** model ***Fluid Flow, Single-phase flow, and Laminar flow***.

2. Channel geometry:

- In Geometry 1, select dimension unit as millimeter "mm".
- Add two *cylinders* of dimensions 10mm (diameter) and 1mm(height) with center at x=0, y=0, z=0 and x=100, y=0, z=0. The *axis* is (x,y,z)=(0,0,1).
- Add a *rectangular* block of dimensions 100mm(width) x 20mm(length) x 1mm(height) with one corner at x=0, y=0, z=0. The *axis* is (x,y,z)=(0,0,1).
- Add two *cylinders* of dimensions 1.5mm (diameter) and 4mm(height) with center at x=0, y=0, z=0 and x=100, y=0, z=0. The *axis* is (x,y,z)=(0,0,1).
- Click *Build All*.

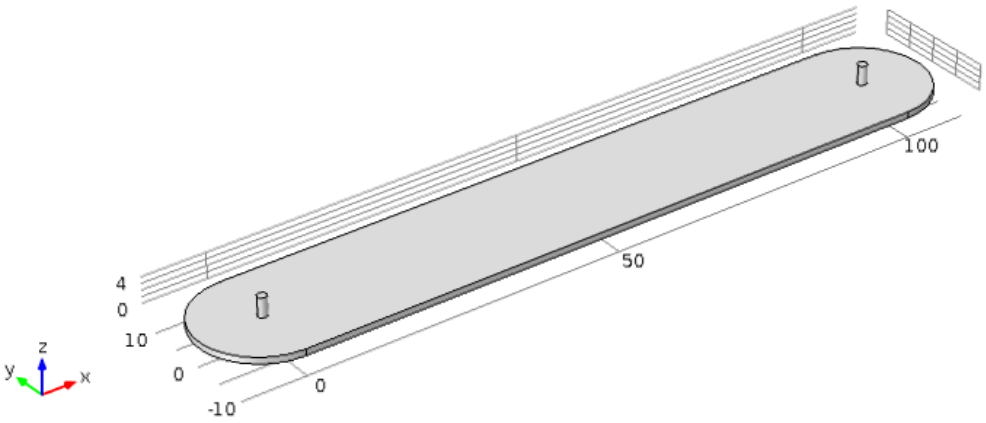

- Similarly, build the grooved channel with channel height 1.5mm and groove depth 1mm. The coordinate for the first grooved shape is x=1,y=-3,z=0 with the width of the groove as 3mm.

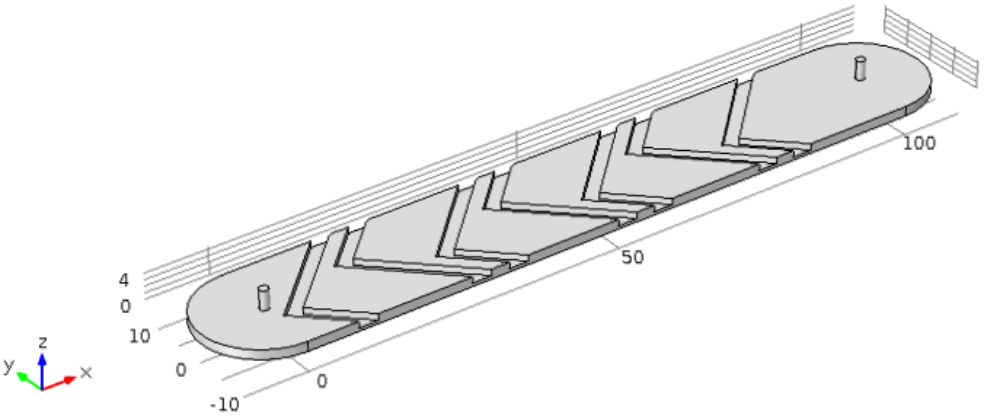

3. Materials:

- Define the channel as "***water, liquid***" from the material library.

4. Laminar flow model set up

- Set *inlet* condition for the top surface of the cylinder with diameter 1.5mm at x=0,y=0,z=0. Select mass flow rate and set it as 2.5e-3[kg/s]
- Set *outlet* condition for the top surface of the cylinder with diameter 1.5mm at x=100,y=0,z=0. Check suppress backflow option.
- Set *wall* condition for the other surfaces of the channel and select no slip condition.

5. Meshing

- Set *Physics controlled mesh* for all domains.
- Set element size as *Fluid dynamics, Fine*. For the subsequent simulations for mesh dependence test change this to *finer*, and *very fine*.
- Click *Build All*

6. Study

- Select *Compute* to solve the model.

7. Post-processing

- In the *Results*, go to *Data sets* and add a surface. Select the bottom surface of the channel and name it as 'bottom'.
- In *Derived values*, go add surface average and name it as 'shear rate'. In the expression type 'spf.sr'. Click on evaluate to obtain the average shear rate on the surface.

- In the *Results*, add a *2D surface plot* and name it as 'shear stress'. Add a *surface* to the plot and select the 'bottom surface' as the *data set*.
- Click on *plot* to obtain the shear rate distribution.

References

[1] D. V. Manov, G. C. Chang, and T. D. Dickey, "Methods for reducing biofouling of moored optical sensors," *J. Atmos. Ocean. Technol.*, vol. 21, no. 6, pp. 958–968, 2004.

[2] A. Whelan and F. Regan, "Antifouling strategies for marine and riverine sensors.," *J. Environ. Monit.*, vol. 8, no. 9, pp. 880–886, 2006.

[3] L. G. Donaruma, W. Characklis, and P. Wilderer, *Structure and function of biofilms*. Wiley Online Library, 1990.

[4] E. Majid, K. B. Male, and J. H. T. Luong, "Boron doped diamond biosensor for detection of Escherichia coli," *J. Agric. Food Chem.*, vol. 56, no. 17, pp. 7691–7695, 2008.

[5] H.-C. Flemming, J. Wingender, and U. Szewzyk, *Springer Series on Biofilms*, vol. 3. 2011.

[6] R. E. Wilson, I. Stoianov, and D. O'Hare, "Biofouling and in situ electrochemical cleaning of a boron-doped diamond free chlorine sensor," *Electrochem. commun.*, vol. 71, pp. 79–83, 2016.

[7] F. Regan, A. Lawlor, B. O. Flynn, J. Torres, R. Martinez-Catala, C. O'Mathuna, and J. Wallace, "A demonstration of wireless sensing for long term monitoring of

water quality," in *2009 IEEE 34th Conference on Local Computer Networks*, 2009, pp. 819–825.

[8] L. Delauney, C. Compare, and M. Lehaitre, "Biofouling protection for marine environmental sensors," *Ocean Sci.*, vol. 6, no. 2, pp. 503–511, 2010.

[9] W. Bourgeois, J. E. Burgess, and R. M. Stuetz, "On-line monitoring of wastewater quality: A review," *J. Chem. Technol. Biotechnol.*, vol. 76, no. 4, pp. 337–348, 2001.

[10] Z. Li, M. J. Deen, S. Kumar, and P. R. Selvaganapathy, "Raman spectroscopy for in-line water quality monitoring—Instrumentation and potential," *Sensors*, vol. 14, no. 9, pp. 17275–17303, 2014.

[11] P. Fowler, D. Baird, R. Bucklin, S. Yerlan, C. Watson, and F. Chapman, "Microcontrollers in Recirculating Aquaculture Systems 1," *Aquaculture*, no. April, pp. 1–7, 1994.

[12] Health Canada, "pH of Drinking Water," 2015. [Online]. Available: http://www.hc-sc.gc.ca/ewh-semt/consult/_2015/ph/draft-ebauche-eng.php.

[13] S. C. Mukopadhyay and A. Mason, *Smart Sensors for Real-Time Water Quality Monitoring*. .

[14] N. Haron, M. Mahamad, I. Aziz, and M. Mehat, "Remote water quality monitoring system using wireless sensors," in *Electronics, Hardware, Wireless and Optical*

Communications, 2009, pp. 148–154.

[15] "Measurement of pH. Definition, standards, and procedures (IUPAC Recommendations 2002) ," *Pure and Applied Chemistry* , vol. 74. p. 2169, 2002.

[16] E. W. Rice, R. B. Baird, A. D. Eaton, L. S. Clesceri, and others, "Standard methods for the examination of water and wastewater," *Am. Public Heal. Assoc. Am. Water Work. Assoc. Water Environ. Fed. Washington, DC*, 2012.

[17] World Health Organization, "pH in Drinking-water," *pH Drink.*, vol. 2, p. 7, 2007.

[18] Fpt Committee On Drinking Water, *Guidelines for Canadian Drinking Water Quality*, no. May 2008. 2008.

[19] Y. Qin, A. U. Alam, M. M. R. Howlader, N. X. Hu, and M. J. Deen, "Inkjet Printing of a Highly Loaded Palladium Ink for Integrated, Low-Cost pH Sensors," *Adv. Funct. Mater.*, vol. 26, no. 27, pp. 4923–4933, 2016.

[20] Y. Qin, A. U. Alam, S. Pan, M. M. R. Howlader, R. Ghosh, P. R. Selvaganapathy, Y. Wu, and M. J. Deen, "Low-temperature solution processing of palladium/palladium oxide films and their pH sensing performance," *Talanta*, vol. 146, pp. 517–524, 2016.

[21] Y. Qin, M. M. R. Howlader, M. J. Deen, Y. M. Haddara, and P. R. Selvaganapathy, "Polymer integration for packaging of implantable sensors," *Sensors Actuators B Chem.*, vol. 202, pp. 758–778, 2014.

[22] H. G. Gorchev and G. Ozolins, "WHO guidelines for drinking-water quality.," *WHO Chron.*, vol. 38, no. 3, pp. 104–108, 2011.

[23] Y. Qin, H.-J. Kwon, M. M. R. Howlader, and M. J. Deen, "Microfabricated electrochemical pH and free chlorine sensors for water quality monitoring: recent advances and research challenges," *RSC Adv.*, vol. 5, no. 85, pp. 69086–69109, 2015.

[24] Y. Qin, H.-J. Kwon, A. Subrahmanyam, M. M. R. Howlader, P. R. Selvaganapathy, A. Adronov, and M. J. Deen, "Inkjet-printed bifunctional carbon nanotubes for pH sensing," *Mater. Lett.*, vol. 176, pp. 68–70, 2016.

[25] Y. Qin, A. U. Alam, M. M. R. Howlader, N.-X. Hu, and M. J. Deen, "Morphology and electrical properties of inkjet-printed palladium/palladium oxide," *J. Mater. Chem. C*, vol. 5, no. 8, pp. 1893–1902, 2017.

[26] Y. Qin, S. Pan, M. M. R. Howlader, R. Ghosh, N.-X. Hu, and M. J. Deen, "Paper-based, hand-drawn free chlorine sensor with poly (3, 4-ethylenedioxythiophene): poly (styrenesulfonate)," *Anal. Chem.*, vol. 88, no. 21, pp. 10384–10389, 2016.

[27] "Water Quality," *Environmental Protection Division*. [Online]. Available: http://www.env.gov.bc.ca/wat/wq/BCguidelines/do/do.htm.

[28] CCME (Canadian Council of Ministers of the Environment), "Canadian Water Quality Guidelines for the Protection of Aquatic Life - Dissolved Oxygen

(Freshwater)," *Can. Environ. Qual. Guidel.*, p. 6, 1999.

[29] J. G. Ibanez, M. Hernandez-Esparza, C. Doria-Serrano, A. Fregoso-Infante, and M. M. Singh, "Dissolved oxygen in water," in *Environmental Chemistry*, Springer, 2008, pp. 16–27.

[30] B. Jones, "Oxygen –The Most Important Water Quality Parameter?" [Online]. Available: http://www.indiana.edu/~clp/documents/water_column/Water_Col_V23N1.pdf.

[31] "Helmholtz-Centre for Environmental Research - UfZ." [Online]. Available: https://www.ufz.de/index.php?en=35455.

[32] "World water monitoring day." [Online]. Available: https://sciencelens.co.nz/2012/09/18/world-water-monitoring-day/.

[33] "Environmental Pollution and Ecotoxicology." [Online]. Available: https://www.fws.gov/raleigh/ec_whats_new.html.

[34] W. Guo, H. H. Ngo, and J. Li, "A mini-review on membrane fouling," *Bioresour. Technol.*, vol. 122, pp. 27–34, 2012.

[35] G. D. Bixler and B. Bhushan, "Biofouling: lessons from nature," *Philos. Trans. R. Soc. A Math. Phys. Eng. Sci.*, vol. 370, no. 1967, pp. 2381–2417, 2012.

[36] H.-C. Flemming, "Biofouling in water systems--cases, causes and countermeasures," *Appl. Microbiol. Biotechnol.*, vol. 59, no. 6, pp. 629–640, 2002.

[37] M. W. Shinwari, M. J. Deen, and D. Landheer, "Study of the electrolyte-insulator-semiconductor field-effect transistor (EISFET) with applications in biosensor design," *Microelectron. Reliab.*, vol. 47, no. 12, pp. 2025–2057, 2007.

[38] M. J. Deen, M. W. Shinwari, J. C. Ranuárez, and D. Landheer, "Noise considerations in field-effect biosensors," *J. Appl. Phys.*, vol. 100, no. 7, p. 74703, 2006.

[39] J. J. James Walker, Susanne Surman, *Industrial Biofouling: Detection, Prevention and Control*. 2000.

[40] D. Landheer, G. Aers, W. R. McKinnon, M. J. Deen, and J. C. Ranuarez, "Model for the field effect from layers of biological macromolecules on the gates of metal-oxide-semiconductor transistors," *J. Appl. Phys.*, vol. 98, no. 4, p. 44701, 2005.

[41] D. Landheer, W. R. McKinnon, G. Aers, W. Jiang, M. J. Deen, and M. W. Shinwari, "Calculation of the response of field-effect transistors to charged biological molecules," *IEEE Sens. J.*, vol. 7, no. 9, pp. 1233–1242, 2007.

[42] M. Waleed Shinwari, M. Jamal Deen, E. B. Starikov, and G. Cuniberti, "Electrical conductance in biological molecules," *Adv. Funct. Mater.*, vol. 20, no. 12, pp. 1865–1883, 2010.

[43] M. W. Shinwari, D. Zhitomirsky, I. A. Deen, P. R. Selvaganapathy, M. J. Deen, and D. Landheer, "Microfabricated reference electrodes and their biosensing

applications," *Sensors*, vol. 10, no. 3, pp. 1679–1715, 2010.

[44] S. Safari, P. R. Selvaganapathy, and M. J. Deen, "Microfluidic reference electrode with free-diffusion liquid junction," *J. Electrochem. Soc.*, vol. 160, no. 10, pp. B177--B183, 2013.

[45] S. Safari, P. R. Selvaganapathy, A. Derardja, and M. J. Deen, "Electrochemical growth of high-aspect ratio nanostructured silver chloride on silver and its application to miniaturized reference electrodes," *Nanotechnology*, vol. 22, no. 31, p. 315601, 2011.

[46] A. U. Kamath, J. S. Leach, Y. Li, D. Rong, S. Saint, P. C. Simpson, and M. Brister, "Analyte sensor." Google Patents, 2016.

[47] J. Bartram, R. Ballance, M. Meybeck, E. Kuusisto, A. Mäkelä, and E. Mälkki, "Water Quality," *Water Qual. Monit. -A Pract. Guid. to Des. Implement. Freshw. Qual. Stud. Monit. Program.*, pp. 1–22, 1996.

[48] M. Lehaitre and C. Compère, *Real-Time Coastal Observing Systems for Marine Ecosystem Dynamics and Harmful Algal Blooms: Theory, instrumentation and modelling*. 2008.

[49] L. M. Granhag, J. A. Finlay, P. R. Jonsson, J. A. Callow, and M. E. Callow, "Roughness-dependent removal of settled spores of the green alga Ulva (syn. Enteromorpha) exposed to hydrodynamic forces from a water jet," *Biofouling*, vol.

20, no. 2, pp. 117–122, 2004.

[50] M. Lizotte, C. Hoffman, D. Lechleiter, and J. McDonald, "Wiper and brush device for cleaning water quality sensors." Google Patents, 2004.

[51] G. A. Edgerton, "Oceanographic sensor with in-situ cleaning and bio-fouling prevention system." Google Patents, 1978.

[52] M. Rahmoune and M. Latour, "Application of mechanical waves induced by piezofilms to marine fouling prevention," *J. Intell. Mater. Syst. Struct.*, vol. 7, no. 1, pp. 33–43, 1996.

[53] J. F. Baxter Jr, "Anti-fouling apparatus for marine applications." Google Patents, 2001.

[54] W. Garner III, "Submergible optical sensor housing with protective shutter and methods of operation and manufacture." Google Patents, 2000.

[55] C. Alzieu, "Tributyltin: case study of a chronic contaminant in the coastal environment," *Ocean Coast. Manag.*, vol. 40, no. 1, pp. 23–36, 1998.

[56] B. Antizar-Ladislao, "Environmental levels, toxicity and human exposure to tributyltin (TBT)-contaminated marine environment. A review," *Environ. Int.*, vol. 34, no. 2, pp. 292–308, 2008.

[57] S. M. Evans, "TBT or not TBT?: that is the question," *Biofouling*, vol. 14, no. 2, pp. 117–129, 1999.

[58] H. J. A. Breur, *Fouling and bioprotection of metals: monitoring and control of deposition processes in aqueous environments*. TU Delft, Delft University of Technology, 2001.

[59] D. Soldo, R. Hari, L. Sigg, and R. Behra, "Tolerance of Oocystis nephrocytioides to copper: intracellular distribution and extracellular complexation of copper," *Aquat. Toxicol.*, vol. 71, no. 4, pp. 307–317, 2005.

[60] S. Rajagopal, G. der Velde, M. der Gaag, and H. A. Jenner, "Laboratory evaluation of the toxicity of chlorine to the fouling hydroid Cordylophora caspia," *Biofouling*, vol. 18, no. 1, pp. 57–64, 2002.

[61] J. Kim, Y. Chung, D. Shin, M. Kim, Y. Lee, Y. Lim, and D. Lee, "Chlorination by-products in surface water treatment process," *Desalination*, vol. 151, no. 1, pp. 1–9, 2003.

[62] J. Zheng, C. Feng, and T. Matsuura, "Study on reduction of inorganic membrane fouling by ultraviolet irradiation," *J. Memb. Sci.*, vol. 244, no. 1, pp. 179–182, 2004.

[63] E. R. Blatchley, K. C. Bastian, R. K. Duggirala, J. E. Alleman, M. Moore, and P. Schuerch, "Ultraviolet irradiation and chlorination/dechlorination for municipal wastewater disinfection: Assessment of performance limitations," *Water Environ. Res.*, vol. 68, no. 2, pp. 194–204, 1996.

[64] K. Nandakumar, H. Obika, T. Shinozaki, T. Ooie, A. Utsumi, and T. Yano, "Pulsed laser irradiation impact on two marine diatoms Skeletonema costatum and Chaetoceros gracilis," *Water Res.*, vol. 37, no. 10, pp. 2311–2316, 2003.

[65] K. Nandakumar, H. Obika, T. Shinozaki, T. Ooie, A. Utsumi, and T. Yano, "Lethal and sub-lethal impacts of pulsed laser irradiations on the larvae of the fouling barnacle Balanus amphitrite," *Biofueling*, vol. 19, no. 3, pp. 169–176, 2003.

[66] F. Mermillod-Blondin, G. Fauvet, A. Chalamet, and M. des Châtelliers, "A comparison of two ultrasonic methods for detaching biofilms from natural substrata," *Int. Rev. Hydrobiol.*, vol. 86, no. 3, pp. 349–360, 2001.

[67] T. R. Bott and L. Tianqing, "Ultrasound enhancement of biocide efficiency," *Ultrason. Sonochem.*, vol. 11, no. 5, pp. 323–326, 2004.

[68] B. G. Pound, Y. Gorfu, P. Schattner, and K. E. Mortelmans, "Ultrasonic mitigation of microbiologically influenced corrosion," *Corrosion*, vol. 61, no. 5, pp. 452–463, 2005.

[69] T. R. Bott, *Fouling of heat exchangers*. Elsevier, 1995.

[70] N. Oulahal-Lagsir, A. Martial-Gros, M. Bonneau, and L. J. Blum, "'Escherichia coli-milk' biofilm removal from stainless steel surfaces: Synergism between ultrasonic waves and enzymes," *Biofueling*, vol. 19, no. 3, pp. 159–168, 2003.

[71] K. Manmaru and T. Shimono, "Ocean environment monitoring system and method for controlling the same." Google Patents, 1997.

[72] T. Nakayama, H. Wake, K. Ozawa, H. Kodama, N. Nakamura, and T. Matsunaga, "Use of a titanium nitride for electrochemical inactivation of marine bacteria," *Environ. Sci. Technol.*, vol. 32, no. 6, pp. 798–801, 1998.

[73] C. E. Nebel, B. Rezek, D. Shin, H. Uetsuka, and N. Yang, "Diamond for bio-sensor applications," *J. Phys. D. Appl. Phys.*, vol. 40, no. 20, p. 6443, 2007.

[74] C.-F. de Lannoy, D. Jassby, K. Gloe, A. D. Gordon, and M. R. Wiesner, "Aquatic biofouling prevention by electrically charged nanocomposite polymer thin film membranes," *Environ. Sci. Technol.*, vol. 47, no. 6, pp. 2760–2768, 2013.

[75] L. G. Spears, J. H. Stone, and E. Klein, "Electrolysis of copper screening: a technique for the prevention of marine fouling," *Environ. Sci. Technol.*, vol. 3, no. 6, pp. 576–580, 1969.

[76] S. Ahmad, *Food Processing: Strategies for Quality Assessment*. 2014.

[77] L. K. Wang, J. P. Chen, Y.-T. Jung, and N. K. Shammas, *Membrane and Desalination Technologies*, vol. 13. 2008.

[78] A. Basile, A. Cassano, and N. K. Rastogi, *Advances in membrane technologies for water treatment: Materials, processes and applications*. Elsevier, 2015.

[79] S. P. Nunes and K.-V. Peinemann, *Membrane technology*. Wiley Online Library,

2001.

[80] N. N. Li, A. G. Fane, W. S. W. Ho, and T. Matsuura, *Advanced membrane technology and applications*. John Wiley & Sons, 2011.

[81] J. Mulder, *Basic principles of membrane technology*. Springer Science & Business Media, 2012.

[82] S. Abrahamsson, *Structure of biological membranes*, vol. 34. Springer Science & Business Media, 2013.

[83] L. I. Rothfield, *Structure and function of biological membranes*. Academic Press, 2014.

[84] R. W. Baker, *Membrane technology*. Wiley Online Library, 2000.

[85] V. S. Kislik and others, *Liquid membranes: principles and applications in chemical separations and wastewater treatment*. Elsevier, 2009.

[86] R. Baker, "Membrane technology in the chemical industry: future directions," *Membr. Technol. Chem. Ind.*, pp. 268–295, 2001.

[87] W. Eykamp, "Microfiltration and ultrafiltration," *Membr. Sci. Technol.*, vol. 2, pp. 1–43, 1995.

[88] S. B. S. Ghayeni, P. J. Beatson, A. J. Fane, and R. P. Schneider, "Bacterial passage through microfiltration membranes in wastewater applications," *J. Memb. Sci.*, vol. 153, no. 1, pp. 71–82, 1999.

[89] P. Wu and M. Imai, "Novel Biopolymer Composite Membrane Involved with Selective Mass Transfer and Excellent Water Permeability," *Adv. Desalin.*, pp. 57–81, 2012.

[90] R. Bian, K. Yamamoto, and Y. Watanabe, "The effect of shear rate on controlling the concentration polarization and membrane fouling," *Desalination*, vol. 131, no. 1–3, pp. 225–236, 2000.

[91] N. Lee, G. Amy, J. P. Croue, and H. Buisson, "Identification and understanding of fouling in low-pressure membrane (MF/UF) filtration by natural organic matter (NOM)," *Water Res.*, vol. 38, no. 20, pp. 4511–4523, 2004.

[92] J. G. Jacangelo, R. Rhodes Trussell, and M. Watson, "Role of membrane technology in drinking water treatment in the United States," *Desalination*, vol. 113, no. 2–3, pp. 119–127, 1997.

[93] S. Popović, D. Jovičević, M. Muhadinović, S. Milanović, and M. N. Tekić, "Intensification of microfiltration using a blade-type turbulence promoter," *J. Memb. Sci.*, vol. 425–426, pp. 113–120, 2013.

[94] F. Lipnizki, "Cross-Flow Membrane Applications in the Food Industry," *Membr. Technol.*, vol. 3, pp. 1–24, 2010.

[95] C. M. K. Muthukumarappan, "Application of Membrane Separation Technology for Developing Novel Dairy Food Ingredients," *J. Food Process. Technol.*, vol. 4,

no. 9, 2013.

[96] H. Strathmann, L. Giorno, and E. Drioli, *Introduction to membrane science and technology*, vol. 544. Wiley-VCH Weinheim, 2011.

[97] R. R. Bhave, "A cross flow filtration apparatus," *Filtr. + Sep.*, vol. 37, no. 6, p. 29, 2000.

[98] R. W. Field, D. Wu, J. A. Howell, and B. B. Gupta, "Critical flux concept for microfiltration fouling," *J. Memb. Sci.*, vol. 100, no. 3, pp. 259–272, 1995.

[99] C. Alvarado, K. Farris, and J. Kilduff, *Membrane Fouling , Modelling and Recent Developments for Mitigation*. Elsevier B.V., 2016.

[100] W. Yuan and A. L. Zydney, "Humic acid fouling during ultrafiltration," *Environ. Sci. Technol.*, vol. 34, no. 23, pp. 5043–5050, 2000.

[101] A. . Fallis, "Cross Flow Filtration Method Handbook," *J. Chem. Inf. Model.*, vol. 53, no. 9, pp. 1689–1699, 2013.

[102] Sigma Aldrich, "Yeast Extract." [Online]. Available: http://www.sigmaaldrich.com/catalog/product/sigma/y1625. [Accessed: 06-Feb-2017].

[103] M. Nystrom, K. Ruohomaki, and L. Kaipia, "Humic acid as a fouling agent in filtration," *Desalination*, vol. 106, no. 1–3, pp. 79–87, 1996.

[104] F. . Stevenson, *Humus Chemistry: Genesis, Composition, Reactions*. New York:

John Wiley & Sons, 1994.

[105] W. M. Company, "Peristaltic pump." [Online]. Available: http://www.wmcpumps.co.uk/. [Accessed: 08-Nov-2016].

[106] Ohaus, "Digital scale 2001." [Online]. Available: http://scaleman.com/ohaus-sp2001-scoutpro-portable-digital-weighing-scale.html. [Accessed: 08-Nov-2016].

[107] H. T. S. Britton and A. R. Robinson, "CXCVIII.—Universal buffer solutions and the dissociation constant of veronal," *J. Chem. Soc.*, no. 1456, pp. 1456–1462, 1931.

[108] L. Hsu, P. R. Selvaganapathy, J. Brash, Q. Fang, C. Q. Xu, M. J. Deen, and H. Chen, "Development of a low-cost hemin-based dissolved oxygen sensor with anti-biofouling coating for water monitoring," *IEEE Sens. J.*, vol. 14, no. 10, pp. 3400–3407, 2014.

[109] R. Philip-Chandy, P. J. Scully, P. Eldridge, H. J. Kadim, M. G. Grapin, M. G. Jonca, M. G. D'Ambrosio, and F. Colin, "An optical fiber sensor for biofilm measurement using intensity modulation and image analysis," *IEEE J. Sel. Top. Quantum Electron.*, vol. 6, no. 5, pp. 764–772, 2000.

[110] A. R. Costa, M. N. de Pinho, and M. Elimelech, "Mechanisms of colloidal natural organic matter fouling in ultrafiltration," *J. Memb. Sci.*, vol. 281, no. 1–2, pp. 716–725, 2006.

[111] H. Lee, G. Amy, J. Cho, Y. Yoon, S. H. Moon, and I. S. Kim, "Cleaning strategies for flux recovery of an ultrafiltration membrane fouled by natural organic matter," *Water Res.*, vol. 35, no. 14, pp. 3301–3308, 2001.

[112] Z. Wang, Y. Zhao, J. Wang, and S. Wang, "Studies on nanofiltration membrane fouling in the treatment of water solutions containing humic acids," *Desalination*, vol. 178, no. 1–3 SPEC. ISS., pp. 171–178, 2005.

[113] C.-C. Liu, D. B. Bocchicchio, P. A. Overmyer, and M. R. Neuman, "A palladium-palladium oxide miniature pH electrode," *Science (80-.).*, vol. 207, no. 4427, pp. 188–189, 1980.

[114] S. M. Reddy and P. M. Vadgama, "Surfactant-modified poly(vinyl chloride) membranes as biocompatible interfaces for amperometric enzyme electrodes," *Anal. Chim. Acta*, vol. 350, no. 1–2, pp. 77–89, 1997.

[115] J. Liu, Z. Liu, X. Xu, and F. Liu, "Saw-tooth spacer for membrane filtration: Hydrodynamic investigation by PIV and filtration experiment validation," *Chem. Eng. Process. Process Intensif.*, vol. 91, pp. 23–34, 2015.

[116] G. A. Fimbres-Weihs and D. E. Wiley, "Review of 3D CFD modeling of flow and mass transfer in narrow spacer-filled channels in membrane modules," *Chem. Eng. Process. Process Intensif.*, vol. 49, no. 7, pp. 759–781, 2010.

[117] S. S. Bucs, A. I. Radu, V. Lavric, J. S. Vrouwenvelder, and C. Picioreanu, "Effect

of different commercial feed spacers on biofouling of reverse osmosis membrane systems: A numerical study," *Desalination*, vol. 343, pp. 26–37, 2014.

[118] P. Xie, L. C. Murdoch, and D. A. Ladner, "Hydrodynamics of sinusoidal spacers for improved reverse osmosis performance," *J. Memb. Sci.*, vol. 453, pp. 92–99, 2014.

[119] P. Yue, C. ZHOU, and J. J. Feng, "Chaotic Mixer for Microchannels," *J. Fluid Mech.*, vol. 645, no. 5555, p. 279, 2010.

[120] S. L. Stott, C.-H. C.-H. Hsu, D. I. Tsukrov, M. Yu, D. T. Miyamoto, B. a. Waltman, S. M. Rothenberg, A. M. Shah, M. E. Smas, G. K. Korir, F. P. Floyd, A. J. Gilman, J. B. Lord, D. Winokur, S. Springer, D. Irimia, S. Nagrath, L. V. Sequist, R. J. Lee, K. J. Isselbacher, S. Maheswaran, D. a. Haber, and M. Toner, "Isolation of circulating tumor cells using a," *October*, vol. 107, no. 35, pp. 18392–7, 2010.

[121] N. S. L. Jr and J. Homola, "Biosensor Enhancement Using Grooved Micromixers : Part I , Numerical Studies Supplementary Information Abstract S-1 S-2," vol. 12, pp. 1–8.

[122] N. S. Lynn, M. Bocková, P. Adam, and J. Homola, "Biosensor Enhancement Using Grooved Micromixers: Part II, Experimental Studies," *Anal. Chem.*, p. 150521092112006, 2015.

[123] P. Sundararajan and A. D. Stroock, "Transport Phenomena in Chaotic Laminar Flows," *Annu. Rev. Chem. Biomol. Eng.*, vol. 3, no. 1, pp. 473–496, 2012.

[124] J. Liu, Z. Liu, F. Liu, W. Wei, Z. Li, X. Wang, C. Dong, and X. Xu, "The application of saw-tooth promoter for flat sheet membrane filtration," *Desalination*, vol. 359, pp. 149–155, 2015.